**Region 2**
**UNIVERSITY TRANSPORTATION RESEARCH CENTER**

# Final Report

# Diesel Ultrafine/Fine Particle Emissions in Numbers: Statistical Modeling and Evaluation of Engine Operating Variables


**Prepared by**

**Yiannis Kamarianakis**
**School of Civil and Environmental Engineering**
**Cornell University**

**&**

**Huaizhu Oliver Gao**
**School of Civil and Environmental Engineering**
**Cornell University**
**220 Hollister Hall**
**Ithaca, NY 14853**
**http://www.cee.cornell.edu/contact/index.cfm**


**December 10, 2009**

**Disclaimer**

The contents of this report reflect the views of the authors, who are responsible for the facts and the accuracy of the information presented herein. The contents do not necessarily reflect the official views or policies of the UTRC or the Federal Highway Administration. This report does not constitute a standard, specification or regulation. This document is disseminated under the sponsorship of the Department of Transportation, University Transportation Centers Program, in the interest of information exchange. The U.S. Government assumes no liability for the contents or use thereof.

TECHNICAL REPORT STANDARD TITLE PAGE

| 1. Report No. | 2. Government Accession No. | 3. Recipient's Catalog No. |
|---|---|---|
| | | |

**4. Title and Subtitle**

Diesel ultrafine/fine particle emissions in numbers: Statistical modeling and evaluation of engine operating variables

5. Report Date

6. Performing Organization Code

**7. Author(s)**

Yiannis Kamarianakis & Oliver Gao, Cornell University

8. Performing Organization Report No.
49777-33-19

**9. Performing Organization Name and Address**

Cornell University
220 Hollister Hall
Ithaca, New York 14853

10. Work Unit No.

11. Contract or Grant No.

**12. Sponsoring Agency Name and Address**

University Transportation Research Center
City College of New York
New York, NY 10031

13. Type of Report and Period Covered
Final Report
01/01/09 – 12/31/09

14. Sponsoring Agency Code

15. Supplementary Notes


16. Abstract

This work aims to develop statistical models for ultrafine/fine particle number emission rates from a diesel bus, to evaluate the explanatory power of engine operating variables. Emissions were recorded by using on-board instrumentation in two types of real-world driving conditions: a freeway commuting route and a within-city-limits bus route, with stop and go due to intersections and bus stops. To reduce the risk of drawing spurious conclusions, three replications of the experiment were performed and linear models were estimated using the robust-to-outliers quantile regression method. The set of explanatory covariates examined includes engine speed, engine load percentage, fuel to air ratio, injection pressure, boost pressure and exhaust temperature; statistical models were corrected for variations in ambient temperature.



17. Key Words

Ultrafine Particles, Quantile Regression, Statistical Model, Emission, Linear Model.


18. Distribution Statement

| 19. Security Classif (of this report) | 20. Security Classif. (of this page) | 21. No of Pages | 22. Price |
|---|---|---|---|
| Unclassified | Unclassified | 48 | |

**Form DOT F 1700.7** (8-69)

# Diesel ultrafine/fine particle emissions in numbers: Statistical modeling and evaluation of engine operating variables.

*YIANNIS KAMARIANAKIS* AND H. OLIVER GAO*

Department of Civil and Environmental Engineering, Cornell University, 220 Hollister Hall, Ithaca, New York 14853

ik89@cornell.edu; hg55@cornell.edu

Submitted to *Environmental Science and Technology*

* Corresponding author phone: (607) 330-4387; fax: (607) 255-9004

**Abstract:** This work aims to develop statistical models for ultrafine/fine particle number emission rates from a diesel bus, to evaluate the explanatory power of engine operating variables. Emissions were recorded by using on-board instrumentation in two types of real-world driving conditions: a freeway commuting route and a within-city-limits bus route, with stop and go due to intersections and bus stops. To reduce the risk of drawing spurious conclusions, three replications of the experiment were performed and linear models were estimated using the robust-to-outliers quantile regression method. The set of explanatory covariates examined includes engine speed, engine load percentage, fuel to air ratio, injection pressure, boost pressure and exhaust temperature; statistical models were corrected for variations in ambient temperature.

## Introduction

A large number of published epidemiologic studies that examine health effects of particulate matter (PM) air pollution conclude that fine combustion-source PM pollution, common to many urban and industrial environments, is an important risk factor for cardiopulmonary disease (*1*), ischemic heart disease and lung cancer death (*2-4*). Chronic exposure studies suggest relatively broad susceptibility to cumulative effects of long-term repeated exposure to fine particulate pollution, resulting in substantive estimates of population average loss of life expectancy in highly polluted environments (*5*). As noted by Eastwood (*6*), PM10 (particles with aerodynamic diameters smaller than 10 microns) exceedances in the USA continue to affect 21 million people and PM2.5 (particle diameter smaller than 2.5 microns) exceedances continue to affect 53 million people (*7*).

Previous research works have conclusively shown that motor vehicle emissions constitute the major source of fine/ultrafine particle pollution in urban environments (*8-10*). A large fraction of these particles come from heavy duty diesel vehicles (*11*). For instance, Kirchstetter et al. (*12*) measured particle emissions from light and heavy duty vehicles in a roadway tunnel and showed that heavy duty diesel trucks emitted 24 times more fine particle mass per unit fuel mass burned than light duty vehicles; heavy duty vehicles also emitted 15–20 times the number of particles per unit mass of fuel burned compared to light duty vehicles.

The vast majority of studies that aimed at estimating relationships between PM emissions and engine operating or vehicle operating variables, has modeled and predicted mass concentrations (*13*). However, evidence now suggests that particulate matter number concentration may provide more insight into the health risks of PM emissions as the particles of most concern are small enough to lodge deep in the lungs where they can do serious damage (*14*). Harmful small particles, account for over 90% of the number-based concentrations, while having negligible mass (*6*). Thus, they are relatively unnoticed in

PM mass measurements, compared to the less numerous, large mass counterparts. Moreover, fine/ultrafine particles –due to their overwhelming numbers- have a high surface area relative to coarse particles, which allows them to "carry considerable amounts of air toxics" (*15*).

Consequently, to provide added insight on the health impact of motor vehicle exhaust, substantial research has been conducted to evaluate particle number emissions from gasoline and diesel vehicles, in both laboratory (*16, 17*) and roadway tests (*18, 19*). A few studies analyzed high frequency PM number data under the transient driving conditions experienced in the real world (*20-24*) aiming at better understanding the relationship between driving modes and PM emissions. It has been reported that measured particle number concentrations differ substantially between real world driving and laboratory tests. Existing modal emission modeling approaches, designed to estimate transient vehicular emissions based on vehicle operating variables like speed and acceleration, did not provide satisfactory predictive power for PM number concentration *(24*).

This work aims at evaluating the effects of engine operating variables on ultrafine/fine particle number emission rates (number of particles per second) for a heavy duty vehicle with a diesel engine, under real-world driving conditions. High frequency data from a diesel transit bus are analyzed for two modes of driving operation: driving in a freeway commuting route and driving in a typical within-city-limits bus route, with stop-and-go due to intersections and simulated bus stops. We reduce the risk of drawing spurious conclusions by analyzing data for three replications for each route and examining the variability of estimated effects of the explanatory variables per route.

In contrast to particle volume or mass measurements, particle numbers are very sensitive to a number of factors, the most important ones being related to dilution conditions (*11*). Thus, some outlying and erroneous observations can be expected from experiments like the one conducted in this study. To minimize the effects of such observations in our estimations, the robust-to–outliers quantile regression modeling framework has been adopted (*25*). It is noteworthy that via this semi-parametric modeling

approach, more sensible, free from distributional assumptions, confidence intervals for the predictions of PM number rates can be constructed. The estimated models are built after letting the data determine the functional transformations that result in a linear relationship between the dependent variables and the covariates. Although the data used are specific to the buses tested, the adopted robust statistical modeling approach can be applied to modeling emissions from other vehicle models with different engine types, exhaust systems and engine retrofit technologies, in a straightforward manner.

## The Experiment

The dataset analyzed in this study is part of a database constructed by Holmén et al. (*21, 26*) for a large experiment that aimed to test for PM emissions differences between conventional diesel and hybrid diesel-electric buses, under different driving modes and fuel/aftertreatment configurations. Other parts of this database have been previously analyzed with statistical procedures by Sonntag et al. (*22, 23*) and Sonntag and Gao (*27*). In this work, we focus on data obtained from a conventional diesel bus that was a member of the Connecticut Transit bus fleet when the experiments by Holmén et al. (*21*) were conducted. The bus was equipped with a 2002 Detroit Diesel Series 40 engine which was certified to meet EPA PM emissions standards, a diesel oxidation catalyst, and had a 40 foot New Flyer chassis. The bus ran on #1 diesel fuel which had sulfur content between 230 and ~320 ppm. A single driver was used throughout the experiment. For the data set analyzed in this study the bus was subject to on-board testing under the above mentioned fuel/aftertreatment configuration for three days: 28 April 2004, 26 and 27 May 2004.

This work examines on-board testing data for two bus routes in Hartford, CT: Enfield and Farmington. Enfield is a freeway commuting route, 16.4 miles in length. The average speed while driving in Enfield route was 61.1 mi/hr, the average load percentage was 79.7%, acceleration ranged from -1 to 0.75 mph/s, grade ranged from -5.6% to 3.1% while the average percentage of idle time was equal to 0.5%. The Farmington route runs 5.2 miles through downtown Hartford, with stop-and-go driving conditions due to intersections and simulated bus stops. The average speed while driving in

Farmington route was 6.79 mi/hr, the average engine load percentage was 49.9%, acceleration rates ranged from -5.1 to 3.3 mph/s, grade ranged from -6.7% to 5.6% while the average percentage of idle time was equal to 34.3%. After an initial warm-up run on each testing day, the bus routes were tested in outbound and inbound runs. The results presented in this study correspond to the inbound runs; statistical analyses of the data that correspond to the outbound runs revealed similar outcomes to the inbound runs and will not presented here for brevity. Data that correspond to the warm-up period were discarded.

A sample of the exhaust was diluted in a mini dilution tunnel with dilution ratios that ranged from 22 to 35. Particle numbers were measured by an Electrical Low Pressure Impactor (ELPI); the ELPI measured particle counts with 12 size cuts for a particle size range between 7nm and 10060nm at a temporal resolution of 1~2 seconds. The particle counts within the first 3 size cuts (7nm to 95.1nm) were summed to determine the total number of ultrafine particles emitted. The counts within the next 7 size cuts (95.1nm to 2420nm) were summed to determine the total number of fine particles (ultrafine particles being excluded), whereas the sum of the counts in the last two size cuts (2420nm to 10060nm) determined the total number of coarse particles emitted (fine and ultrafine particles being excluded). The analysis that corresponds to coarse particles will not be presented in this article for reasons that will be clarified in the following sections.

Data on engine operating variables were collected from a Vansco data link adapter connected to the network port of the bus. The following engine operating variables were examined: load percentage (%), engine speed (rpm), fuel to air ratio, exhaust temperature (K), boost pressure (kPa) and injection pressure (MPa). The goal of the statistical analysis that is depicted in the following sections is to capture the variability of emitted ultrafine/fine particles with models that use the above as explanatory variables; functional transformations and interactions of the explanatory variables are considered as well.

A Pitot tube from a Horiba OBS-1000 gas-emission analyzer was employed to measure the total exhaust flow rate at the end of the tailpipe, at a temporal resolution of one-second intervals. To calculate the particle number emission rate, the data from the Horiba and ELPI instruments were time aligned with the data from Vansco to account for the lag caused by the dilution system and different instrument times, according to the procedure documented in (*21*) and (*26*). The ultrafine/fine/coarse particle number emission rate was calculated by multiplication of the corresponding particle number concentration with the total exhaust flow rate and the dilution ratio.

## Particle Numbers and Engine Operating Variables: Exploratory Analysis

### Empirical distributions

The distributions of engine operating variables for the three replications of each route are depicted in the Supporting Information. The number of measurements ranged from 370 to 395 for Enfield route and from 366 to 479 for Farmington route. The figures show that the two routes correspond to substantially different modes of operation. Moreover, they offer an exploratory assessment of between- replication-variability within the same route.

It can be observed that, in accordance with intuition, engine speed is (about 1000 rpm) lower on average while the bus was driven in Farmington route. The interquartile ranges observed for Enfield are very narrow compared to Farmington, indicating low variability around mean rpm levels. Engine speed distributions are close to being symmetric for Enfield whereas they are positively-skewed for Farmington with average levels substantially higher than the corresponding medians. It is noteworthy that the second replication for Enfield route differs with respect to the first and third ones, as it concentrated in higher rpm levels. The observed median rpm for the first replication of Farmington is also substantially increased compared to the medians of the second and third replications which are very close to the lowest rpm levels (which correspond to idling).

Percentages of engine loads are concentrated in the upper half of the sample space for Enfield route whereas they are concentrated at about 50% engine load with a narrow interquartile range (albeit with several outlying observations) for Farmington route. Similar to engine speed, higher loads are observed in the second replication of the Enfield route. Distributions that correspond to fuel to air ratios, injection and boost pressure (see Supporting Information) are concentrated at higher levels in Enfield; moreover, the distributions for Farmington are positively skewed whereas the majority of the ones that correspond to Enfield are negatively skewed. Observed exhaust temperatures for Enfield are almost 100 degrees higher than the ones observed in Farmington. Moreover, substantial differences for ambient temperatures that correspond to different replications of the same route were observed.

Ultrafine particle number emission rates (#/second) are on average about 4 times larger in Enfield with average rates -per replication- that range from $2x10^{11}$ to $3.5x10^{11}$. The distributions observed in Enfield are close to being symmetric; however, the normality assumption is strongly rejected by the Shapiro-Wilk, Carmer von Mises and Anderson-Darling tests for the first and the third replication of the experiment as the calculated p-values were less than 0.01 in magnitude. On the other hand, positively skewed distributions and a relatively large number of outlying observations are observed in Farmington. Finally, it can be observed that fine particle number emission rates are about 10 times lower than the corresponding ultrafine rates. Similar to what was observed for ultrafine particles, rates that correspond to Farmington are about five times lower on average compared to the ones observed in Enfield.

**Correlations**

If ultrafine particle number emission rates were strongly correlated with fine particle number rates, one could evaluate their dependence on engine operating variables via formulating a single statistical model. However, ultrafine particle emission rates were not found strongly correlated with larger particle rates in on-road studies (*28, 29*). A similar finding from the dynamometer tests conducted by Morawska et al. (*30*) suggested that "small and large particle ranges should be tested independently to provide a

comprehensive characterization of the vehicle particle emissions". The findings of this study suggest that correlations vary substantially for the two modes of driving operation. For instance, ultrafine rates are very strongly correlated with fine rates in the low emitting Farmington route with Spearman's correlation coefficients that range from 0.91 to 0.96. On the other hand, only moderate evidence in favor of a linear association was provided in the high emitting Enfield route; Spearman's correlation coefficient ranged from 0.51 to 0.6. Similar to Janhall et al. (*31*), Spearman's nonparametric rank order correlation was used instead of the conventional Pearson's correlation in our investigation, so that extreme values do not affect the associated tests of significance.

Associations of ultrafine/fine emission rates with engine operating variables (see Supporting Information), appear to vary substantially with driving mode as well. For instance, both ultrafine and fine emission rates are more strongly (linearly) associated with engine speed in Farmington –where Spearman's coefficients ranged from 0.79 to 0.87 for ultrafine and from 0.75 to 0.86 for fine particles- than in Enfield, where Spearman's coefficients ranged from 0.23 to 0.62 for ultrafine and from 0 to 0.4 for fine particles.

Engine load was found to be associated more strongly with fine particle emission rates than with ultrafine rates. For fine particles, Spearman's correlation coefficient ranged from 0.77 to 0.79 in Enfield and from 0.44 to 0.57 in Farmington; for ultrafine particles, the corresponding coefficients ranged from 0.15 to 0.34 for Enfield and from 0.4 to 0.51 for Farmington. Fuel to air ratios were also found more strongly (linearly) associated with fine particle emission rates as Spearman's correlation coefficients ranged from 0.69 to 0.82 for Enfield and from 0.75 to 0.79 for Farmington route. The corresponding coefficients for ultrafine rates range from 0.42 to 0.55 for Enfield and from 0.69 to 0.75 for Farmington.

No evidence of positive linear association between injection pressure and ultrafine/fine rates was observed in Farmington route, as correlation coefficients ranged from -0.02 to 0.06 for ultrafine rates and from 0.05 to 0.15 for fine particle rates. For Enfield route correlations increased: Spearman's

coefficients ranged from 0.05 to 0.29 for ultrafine rates and from 0.22 to 0.45 for fine particle rates. The findings for the association between boost pressure and ultrafine/fine emission rates are reversed as the strongest values of the correlation coefficients were observed in Farmington route. The corresponding coefficients range from 0.42 to 0.55 for ultrafine rates and from 0.46 to 0.6 for fine particle emission rates. On the other hand, only moderate evidence in favor of a linear association was observed in Enfield route as coefficients ranged from 0.05 to 0.26 for ultrafine rates and from 0.18 to 0.41 for fine particle rates, respectively.

Moderate evidence in favor of a negative association was observed in Enfield between exhaust temperature and ultrafine particle emission rates: Spearman's coefficients ranged from -0.01 to -0.26. For fine particle rates the coefficients ranged from 0.33 to 0.53. In Farmington route, positive associations were observed in both examined cases: correlation coefficients ranged from 0.19 to 0.26 for the relationship between exhaust temperature and ultrafine rates and from 0.22 to 0.24 for the relationship between exhaust temperature and fine particle rates. This finding is in accordance with intuition, as increased levels of exhaust temperature are usually related to high engine loads and high fuel rates. With regard to the negative correlation observed for ultrafine particle rates in Enfield, it should be noted that after conducting a series of dynamometer tests, Holmén and Ayala (*32*) did not find conclusive evidence for the bivariate association between exhaust temperature and nanoparticle number concentration. On the other hand, Giechaskiel et al. (*33*) concluded that nanoparticle formation requires an exhaust gas temperature range which enhances SO2 to SO3 conversion. As noted by Maricq et al. (*34*) who also examined the effects of exhaust temperature, "artifacts are hard to avoid when measuring particle number and size at high speeds and loads".

**Functional specification for linear model building**

A preliminary analysis before model estimation consisted of a bivariate examination of power transformations that linearize relationships between response variables (e.g. emission rates) and each

one of the engine operating variables. For that purpose, the resistant-to-outliers technique proposed by Tukey (*35*) was applied to the augmented set of explanatory variables to which the interaction between engine load percentage and engine speed was added. Square root transformations were indicated as optimal in the vast majority of the examined bivariate relationships between ultrafine/fine particle number emission rates and engine operating variables. It is noteworthy that the square root transformation, similar to the logarithmic one, is routinely used in applied statistics research for highly positively skewed data and is especially used in transforming Poisson counts to normality (*36*). Logarithmic transformations were found optimal for coarse particle number emission rates. As statistical models for coarse particle number rates would not be directly comparable to the ones that correspond to ultrafine/fine particle number rates if the logarithmic transformation is adopted, the analysis of coarse particles is deferred for a forthcoming publication. Quadratic forms of engine speed and fuel to air ratios were indicated to provide increased explanatory power at this stage of the analysis. The latter observation is consistent with Heywood (*37, chapter 11*). For the remaining explanatory variables, linear relationships were deemed as optimal.

## Quantile Regression Models: Estimation and Discussion

The semiparametric technique of quantile regression introduced by Koenker and Bassett (*38*) has received a lot of attention in both theoretical and applied research during the last thirty years. The quantile regression model extends the notion of ordinary quantiles in a location model, to a more general class of linear models in which the conditional quantiles have a linear form. A special case of quantile regression is the least absolute deviation (LAD) estimator; LAD estimation is potentially attractive compared to ordinary least squares estimation of regression coefficients, for the same reasons that the median may be a better measure of location than the mean.

Some useful features of quantile regression can be summarized as follows (*39*): (a) the models can be used to characterize the entire conditional distribution of a dependent variable given a set of explanatory

variables; (b) the quantile regression model has a linear programming representation which makes estimation easy; (c) like the LAD minimand, the quantile regression objective is a weighted sum of absolute deviations which gives a robust measure of location, so that the estimated coefficient vector is not sensitive to outlying observations on the dependent variable; (d) when the error terms deviate from the normality assumption, quantile regression estimators may be more efficient than least squares estimators; and (e) potentially different solutions at distinct quantiles may be interpreted as differences in the response of the dependent variable to changes in the regressors, at various points in the conditional distribution of the dependent variable. The interested reader may consult Yu et al. (*40*) and Koenker (*25*) for extensive discussions.

Tables 1 and 2 present linear models estimated via LAD for fine particle number rates, following the general-to-specific approach (estimated models for ultrafine number rates are shown in the Supporting Information). The square roots of fine particle number emission rates were the response variables and different models were estimated for each replication of the Enfield/Farmington route. The starting point of the general-to-specific approach is a regression model that includes ten explanatory covariates: engine speed, engine speed squared, fuel to air ratio, fuel to air ratio squared, load percentage, interaction term of load and engine speed, exhaust temperature, boost pressure, injection pressure and ambient temperature. Ambient temperature was centralized and the minimum was subtracted from each of the engine operating variables so that estimated intercepts correspond to a proxy of the square root of observed particle number rates while the bus was idling. Wald tests were performed to test for restrictions in the full model. Only the remaining statistically significant terms (after a series of Wald tests) are displayed in the tables with the exception of ambient temperature which is always included as an explanatory covariate (although its effect was found statistically significant only in six of the twelve estimated models) so that all estimated covariate effects correspond to average temperature.

A first examination of tables 1 and 2 (see also Supporting Information) reveals that covariate effects which remained as significant in the final models, were almost the same between replications for each

of the four, route-class/particle- size emission rates combinations. Moreover, the estimated effects were close in terms of magnitude. It is noteworthy that the interaction of load percentage with engine speed was a significant covariate in all examined models. This finding is consistent with (*27*) who analyzed link-level-aggregated particle numbers using different statistical techniques than the ones adopted here and reported that engine speed and load were the two most effective variables for modeling particle number emissions. Fuel to air ratios were also included as statistically significant explanatory variables in all (12) estimated LAD regression models. On the other hand, injection pressure did not provide sufficient explanatory power to be included in any of the estimated models. Mathis et al. (*41*) report a negative association of injection pressure with particle numbers, especially in low engine loads, a finding which was could not be confirmed from our exploratory and modeling analyses.

Strong evidence in favor of the significance of the effect of exhaust temperature is provided while the bus was driven in the high-emitting Enfield route, for both ultrafine and fine particle number emission rates. However, it appears only once as a significant covariate in models that correspond to Farmington route where exhaust temperatures were significantly lower. One may observe negative coefficients for the effects of exhaust temperature for ultrafine rates in Enfield, which is consistent with what was observed in the exploratory stage of the analysis. Negative effects of exhaust temperature in particle number rates have also been observed in (*27*); according to Kittelson et al. (*19*) such a finding could correspond to an increase in condensation and nucleation of volatile precursors under cooler temperatures.

Engine speed is a significant covariate for particle number emission rates in Farmington route while it is not significant in Enfield; this can be explained by the small variability of engine speed while the bus was driven in Enfield (see Supporting Information). On the contrary, the effects of engine load percentages are only significant in the models that correspond to Enfield; similarly, this can be explained by the small variability of load percentages while the bus was driven in Farmington. Moreover, one may observe that quadratic effects of engine speed appear to be significant for ultrafine

particles whereas they are not significant for fine particle number rates. As shown in the Supporting Information, the effect of engine speed on ultrafine number rates in Farmington, is maximized at about 1450 rpm. Similarly, quadratic effects of fuel to air ratios are only significant for ultrafine particle rates in Enfield. Boost pressure appears as a significant covariate only while the bus was driven in Farmington route. Janhall et al. (*31*) and Sonntag and Gao (*27*) report that ambient temperature correlated negatively with ultrafine particle number rates. This finding could not be confirmed here, as tables 1-4 do not provide conclusive evidence with regard to the sign of the estimated temperature effects.

From tables 1 and 2 one may estimate the effects of a change in any covariate, given fixed values for the remaining ones. For instance, from table 1 which depicts the three estimated LAD regression models for fine particle rates in Enfield, one may deduce that, given that the other engine operating variables are at their minimum levels, a 0.01 increase in fuel to air ratio results in an increase in fine particle numbers which ranges from 370,689 (based on the estimated fuel to air ratio in the second replication of the experiment), to 919,681 (based on the estimated fuel to air ratio in the first replication). On the other hand, based on table 2 (Farmington route), a 0.01 increase in fuel to air ratio results in an estimated increase in fine particle numbers that ranges from 105,625 to 251,001.

The quantile process plots (see Supporting Information) depict the evolution of the effect of each covariate across the conditional quantiles of the distributions of ultrafine/fine particle number rates. Conditional quantiles range from 0.05 to 0.95 and 95% point-wise confidence bands for the quantile regression parameters, based on the heteroscedasticity robust resampling method of He and Hu (*42*) are also shown. Conventional ordinary least squares regression assumes a uniform effect of the covariates across the conditional quantiles. However, one may observe that the effects of exhaust temperature are steadily increasing across the quantiles of the conditional distribution of the square root of ultrafine PM emission rates in Enfield. Decreasing effects of ambient temperature are observed in the conditional distribution of the square root of fine PM emission rates in Enfield while increasing effects of engine

speed across quantiles of the conditional distribution of the square root of fine PM emission rates in Farmington. Based on the covariate effects estimated, for instance for the 0.1 and 0.9 quantiles, robust, free from the normality assumption, confidence intervals for predicted emission rates can be constructed (figure 1).

ACKNOWLEDGMENT This research used on-board bus emissions data collected from Project 05-9 of the Joint Highway Research Advisory Council of the University of Connecticut and the Connecticut Department of Transportation.

SUPPORTING INFORMATION PARAGRAPH. Graphs of the empirical distributions of ultrafine/fine particle number rates and engine operating variables, scatter-plots for bivariate associations, quantile process plots, a plot of the quadratic effects of engine speed in ultrafine particle number rates in Enfield and LAD regression estimates for ultrafine particle number rates in Enfield and Farmington.

**TABLE 1. LAD regression estimates, 95% confidence limits based on the heteroscedasticity robust resampling method of He and Hu (2002), t-statistics and corresponding p-values, for the effects of engine operating variables on the square root of fine particle number emission rates observed in Enfield route. The general-to-specific model building procedure was adopted, based on a series of Wald tests. Three replications of the experiment are examined which correspond to the following days (from top): 04/28/2004, 05/26/2004 and 05/27/2004.**

| *Parameter* | *Estimate* | *Stand. Error* | *95% Conf.* | *Limits* | *t Value* | *Pr > \|t\|* |
|---|---|---|---|---|---|---|
| *Loadpct* | -96.678 | 6.1969 | -108.862 | -84.4936 | -15.6 | <.0001 |
| *Load*rpm* | 0.0812 | 0.0044 | 0.0726 | 0.0899 | 18.51 | <.0001 |
| *FuelAir* | 95886.06 | 4011.313 | 87998.91 | 103773.2 | 23.9 | <.0001 |
| *ExhaustTemp* | 7.6012 | 0.7377 | 6.1507 | 9.0518 | 10.3 | <.0001 |
| *Amb.Temp.* | -56.5869 | 27.0128 | -109.7 | -3.4735 | -2.09 | 0.0368 |
| *Loadpct* | -78.544 | 5.599 | -89.552 | -67.5359 | -14.03 | <.0001 |
| *Load*rpm* | 0.0652 | 0.0036 | 0.0581 | 0.0722 | 18.22 | <.0001 |
| *FuelAir* | 60943.62 | 5132.992 | 50851.82 | 71035.42 | 11.87 | <.0001 |
| *ExhaustTemp* | 18.7394 | 1.2474 | 16.287 | 21.1917 | 15.02 | <.0001 |
| *Amb.Temp* | -182.206 | 27.2037 | -235.69 | -128.722 | -6.7 | <.0001 |
| *Intercept* | 669.0794 | 245.5417 | 186.2165 | 1151.942 | 2.72 | 0.0067 |
| *Loadpct* | -72.9556 | 10.1112 | -92.8394 | -53.0717 | -7.22 | <.0001 |
| *Load*rpm* | 0.062 | 0.0073 | 0.0476 | 0.0764 | 8.47 | <.0001 |
| *FuelAir* | 86674.64 | 4171.203 | 78471.88 | 94877.4 | 20.78 | <.0001 |
| *ExhaustTemp* | 4.6758 | 1.0215 | 2.6669 | 6.6847 | 4.58 | <.0001 |
| *Amb.Temp.* | 14.693 | 56.3592 | -96.1387 | 125.5246 | 0.26 | 0.7945 |

**TABLE 2. LAD regression estimates, 95% confidence limits based on the heteroscedasticity robust resampling method of He and Hu (2002), t-statistics and corresponding p-values, for the effects of engine operating variables on the square root of fine particle number emission rates observed in Farmington route. The general-to-specific model building procedure was adopted, based on a series of Wald tests. Three replications of the experiment are examined which correspond to the following days (from top): 04/28/2004, 05/26/2004 and 05/27/2004.**

| *Parameter* | *Estimate* | *Stand. Error* | *95% Conf.* | *Limits* | *t Value* | *Pr > \|t\|* |
|---|---|---|---|---|---|---|
| *Load*rpm* | 0.0106 | 0.002 | 0.0054 | 0.0158 | 5.26 | <.0001 |
| *EngineSpeed* | 0.7315 | 0.1478 | 0.349 | 1.1141 | 4.95 | <.0001 |
| *FuelAir* | 32561.33 | 5645.339 | 17944.72 | 47177.93 | 5.77 | <.0001 |
| *ExhaustTemp* | 2.4774 | 0.8063 | 0.3896 | 4.5651 | 3.07 | 0.0023 |
| *Boostp* | 3.1529 | 0.6196 | 1.5486 | 4.7571 | 5.09 | <.0001 |
| *Amb.Temp* | 12.7603 | 19.1849 | -36.9123 | 62.4329 | 0.67 | 0.5064 |
| *Load*rpm* | 0.0083 | 0.0015 | 0.0043 | 0.0123 | 5.37 | <.0001 |
| *EngineSpeed* | 0.4189 | 0.1138 | 0.1242 | 0.7136 | 3.68 | 0.0003 |
| *FuelAir* | 67726.09 | 1776.528 | 63125.74 | 72326.44 | 38.12 | <.0001 |
| *Amb.Temp* | 11.5347 | 12.902 | -21.8752 | 44.9446 | 0.89 | 0.3719 |
| *Load*rpm* | 0.0084 | 0.0014 | 0.0046 | 0.0121 | 5.81 | <.0001 |
| *EngineSpeed* | 0.3641 | 0.1053 | 0.0918 | 0.6365 | 3.46 | 0.0006 |
| *FuelAir* | 50128.22 | 2929.232 | 42552.51 | 57703.92 | 17.11 | <.0001 |
| *Boostp* | 1.0874 | 0.3063 | 0.2953 | 1.8796 | 3.55 | 0.0004 |
| *Amb.Temp* | 26.8311 | 3.7393 | 17.1605 | 36.5017 | 7.18 | <.0001 |

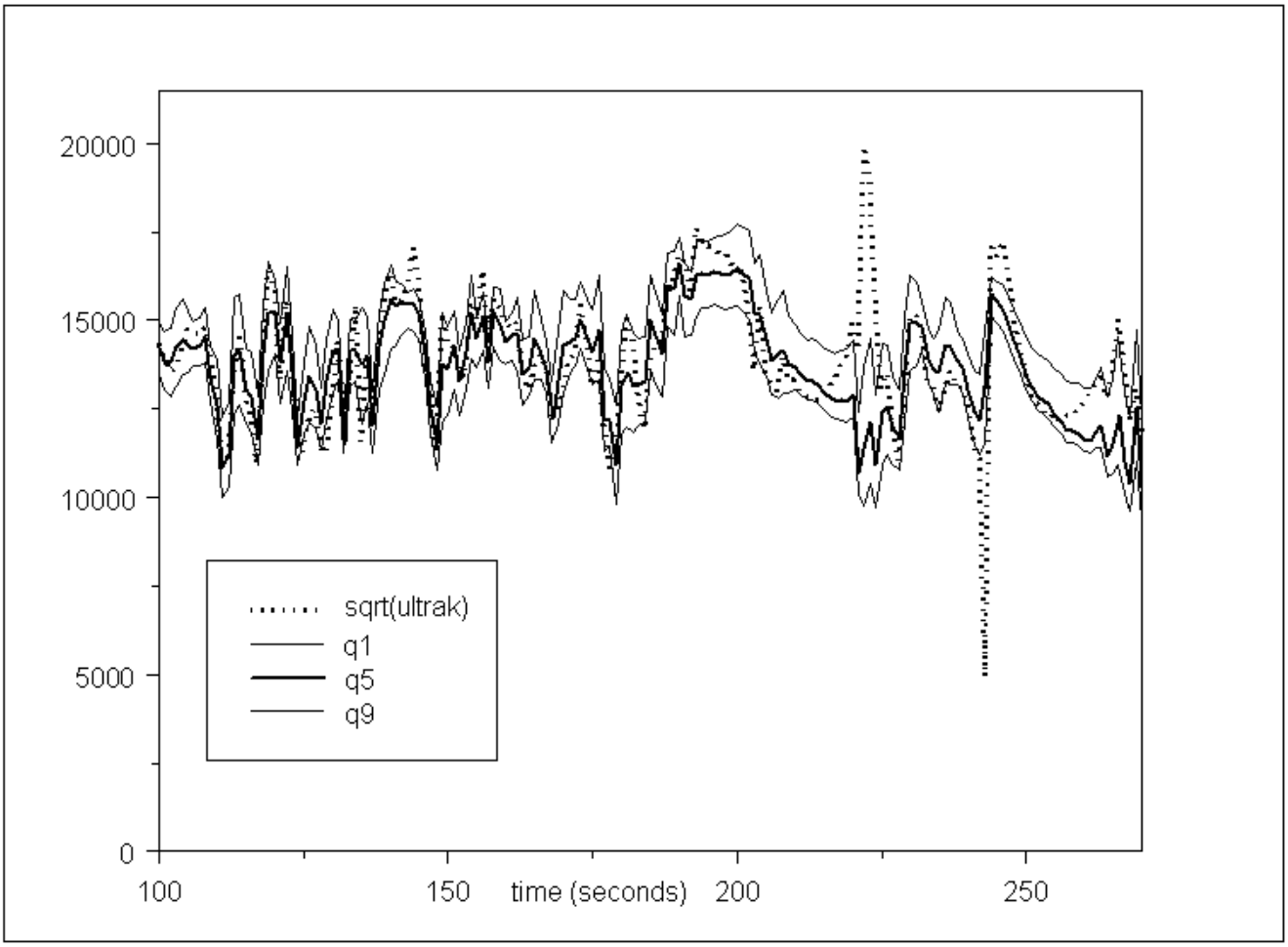


**FIGURE 1. Observed square roots of ultrafine particle number rates (sqrt(ultrak)); predictions based on the 0.5 quantile (q5) and confidence interval formed by the 0.1 (q1) and 0.9 quantiles (q9).**

REFERENCES


(1) Pope, C.A. Review: Epidemiological basis for particulate air pollution health standards. *Aerosol Science and Technology* **2000***, 32*, 4-14.

(2) Pope, C.A.; Burnett, R.T.; Thun, M.T.; Calle, E.E.; Krewski, D.; Kazuhiko, I.; Thurston, G.D. Lung cancer, cardiopulmonary mortality, and long-term exposure to fine particulate air pollution. *Journal of the American Medical Association* **2002***, 287,* 1132-1141.

(3) Jerrett, M.; Burnett, R.T.; Ma, R.; Pope, C.A.; Krewski, D.; Newbold, K.B.; Thurston, G.; Shi, Y.; Finkelstein, N.; Calle, E.E.; Thun, M.J. Spatial analysis of air pollution and mortality in Loa Angeles. *Epidemiology* **2005***, 16,* 727-736.

(4) Ibald-Mulli, A.; Wichmann, H.E.; Kreyling, W.; Peters, A. Epidemiological evidence on health effects of ultrafine particles. *Journal of Aerosol Medicine* **2002***, 15,* 189-201.

(5) Pope, C.A. Epidemiology of fine particulate air pollution and human health: biologic mechanisms and who's at risk? *Environmental Health Perspectives* **2000***, 108,* 713-723.

(6) Eastwood, P. *Particulate emissions from vehicles;* Wiley, 2008.

(7) U.S. EPA. *The particle pollution report-current understanding of air quality and emissions through 2003;* Contract No. 68-D-02-065, Washington D.C., 2004.

(8) Harrison, R.; Jones, M.; Collins, G. Measurements of the physical properties of particles in the urban atmosphere. *Atmospheric Environment* **1999***, 33,* 309–321.

(9) Shi, J.; Harrison, R.M. Investigation of ultrafine particle formation during diesel exhaust dilution. *Environmental Science and Technology* **1999***, 33,* 3730–3736.

(10) Wåhlin, P.; Palmgren, F.; Van Dingenen, R. Experimental studies of ultrafine particles in streets and the relationship to traffic. *Atmospheric Environment* **2001***, 35,* S63–S69.

(11) Morawska, L.; Ristovski, Z.; Jayaratne, E.R.; Keogh, D.U.; Ling, X. Ambient nano and ultrafine particles from motor vehicle emissions: characteristics, ambient processing and implications on human exposure. *Atmospheric Environment* **2008***, 42,* 8113-8138.

(12) Kirchstetter, T.W.; Harley, R.A.; Kreisberg, N.M.; Stolzenberg, M.R.; Hering, S.V. On-road measurement of fine particle and nitrogen oxide emissions from light- and heavy-duty motor vehicles. *Atmospheric Environment* **1999***, 33,* 2955–2968.

(13) North, R.; Noland, R.; Ochieng, W.; Polak, J. Modeling of particulate matter mass emissions from a light-duty diesel vehicle. *Transportation Research Part D: Transport and Environment* **2006***, 11,* 344-357.

(14) American Lung Association. What is particulate matter? http://4cleanair.org, 2004.

(15) Sioutas, C.; Delfino, J.; Singh, M. Exposure assessment for atmospheric ultrafine particles and implications in epidemiologic research. *Environmental Health Perspectives* **2005***, 113,* 947-955.

(16) Zervas, E.; Dorlhene, P.; Daviau, R.; Dionnet, B. Repeatability of fine particle measurement of diesel and gasoline vehicles exhaust gas. SAE Technical Paper Series No. 2004-01-1983.

(17) Mathis, U.; Mohr, M.; Forss, A. Comprehensive particle characterization of modern gasoline and diesel passenger cars at low ambient temperatures. *Atmospheric Environment* **2005***, 39,* 107–117.

(18) Jamriska, M.; Morawska, L.; Thomas, S.; He, C. Diesel bus emissions measured in a tunnel study. *Environmental Science and Technology* **2004***, 38,* 6701–6709.

(19) Kittleson, D.B.; Watts, W.F.; Johnson, J.P. Nanoparticle emissions on Minnesota highways. *Atmospheric Environment* **2004***, 38,* 9–19.

(20) Holmén, B.A.; Qu, Y. Uncertainty in particle number modal analysis during transient operation of compressed natural gas, diesel, and trap-equipped diesel transit buses. *Environmental Science and Technology* **2004***, 38,* 2413-2423.

(21) Holmén, B.A.; Chen, Z.; Davila, A.C.; Gao, O.; Vikara, D.M. *Particulate matter emissions from hybrid diesel-electric and conventional diesel transit buses: Fuel and aftertreatment effects. JHR 05-304 Project 03-8*; Joint Highway Research Advisory Council: Hartford, CT, **2005**.

(22) Sonntag, D.B.; Gao, H.O.; Holmén, B.A. Modeling on-road particle number emissions from a hybrid diesel-electric bus: Exploratory econometric analysis. *Transportation Research Record: Journal of the Transportation Research Board* **2007***, 2011,* 40-48.

(23) Sonntag, D.B.; Gao, H.O.; Holmén, B.A. Variability of particle number emissions from diesel and hybrid diesel-electric buses in real driving conditions. *Environmental Science and Technology* **2008***, 42,* 5637-5643.

(24) Bapat, A.; Gao, H.O. Diesel particulate matter number emissions: evaluation of existing modal emission modeling approaches. *Submitted*, **2009**.

(25) Koenker, R. *Quantile Regression*; Cambridge University Press, 2005.

(26) Holmén, B.A.; Jackson, E.; Sonntag, D.; Gao, O.H. *Detailed modal analysis of particulate emissions from Connecticut Transit buses for local emissions modeling. Draft report prepared for Joint Highway Research Advisory Council Project 05-09*; Joint Highway Research Advisory Council: Hartford, CT, **2008**.

(27) Sonntag, D.B.; Gao, H.O. Developing link-based particle number emission models for diesel transit buses using engine and vehicle parameters. *To appear in Transportation Research Part D: Transport and Environment*, **2009**.

(28) Keywood, M.D.; Ayres, G.P.; Gras, J.P.; Gillett, R.W.; Cohen, D.D. Relationships between size segregated mass concentration data and ultrafine particle number concentrations in urban areas. *Atmospheric Environment* **1999***, 33,* 2907-2913.

(29) Molnar, P.; Janhall, S.; Hallquist, M. Roadside measurements of fine and ultrafine particles at a major road north of Gothenburg. *Atmospheric Environment* **2002***, 36,* 4115-4123.

(30) Morawska, L.; Bofinger, N.D.; Kocis, L.; Nwankwoala, A. Submicrometer and supermicrometer particles from diesel vehicle emissions. *Environmental Science and Technology* **1998***, 32,* 2032-2042.

(31) Janhall, S.; Jonsson, A.S.; Molnar, P.; Svensson, E.A.; Hallquist, M. Size resolved traffic emission factors of submicrometer particles. *Atmospheric Environment* **2004***, 38,* 4331-4340.

(32) Holmén, B.A.; Ayala, A. Ultrafine PM emissions from natural gas, oxidation-catalyst diesel, and particle trap diesel heavy-duty transit buses. *Environmental Science and Technology* **2002***, 36,* 5041-5050.

(33) Giechaskiel, B.; Ntziachristos, L.; Samarias, Z.; Scheer, V.; Casati, R.; Vogt, R. Formation potential of vehicle exhaust nucleation mode particles on-road and in the laboratory. *Atmospheric Environment* **2005***, 39,* 3191-3198.

(34) Maricq, M.M.; Chase, R.E.; Podsiadlik, D.H. Vehicle exhaust particle size distributions: a comparison of tailpipe and dilution tunnel measurements. *SAE Technical Paper 1999-01-1461*, 1-12.

(35) Tukey, J.W. *Exploratory data analysis;* Addison-Wesley Series in Behavioral Science: Quantitative Methods, Reading, Mass.: Addison-Wesley, 1977.

(36) Anscombe, F.J. The transformation of Poisson, Binomial and Negative-Binomial data. *Biometrika* **1948***, 35,* 246-254.

(37) Heywood, J.B. *Internal combustion engine fundamentals;* Mc Graw-Hill: New York, 1988.

(38) Koenker, R.; Bassett, G. Regression Quantiles. *Econometrica* **1978***, 46,* 33-50.

(39) Buchinsky, M. Recent advances in quantile regression models: A practical guideline for empirical research. *The Journal of Human Resources* **1998***, 33,* 88-126.

(40) Yu, K.; Lu, Z.; Stander, J. Quantile regression: applications and current research areas. *Journal of the Royal Statistical Society: Series D (The Statistician)* **2003***, 52,* 331-350.

(41) Mathis, U.; Mohr, M.; Kaegi, R.; Bertola, A.; Boulouchos, K. Influence of diesel engine combustion parameters on primary soot particle diameter. *Environmental Science and Technology* **2005***, 39,* 1887-1892.

(42) He, X.; Hu, F. Markov chain marginal bootstrap. *Journal of the American Statistical Association* **2002***, 97,* 783-795.

**SUPPLEMENTAL INFORMATION**

# Diesel ultrafine/fine particle emissions in numbers: Statistical modeling and evaluation of engine operating variables

Yiannis Kamarianakis, H. Oliver Gao

Summary of Supplemental Information

Total Pages: 26

Number of Figures: 29

Number of Tables: 2

Figures S-1 to S-3 display the distributions of engine operating variables and ultrafine/fine particle number rates per replication of each route. Figures S-4 to S-16 are scatter-plots for the bivariate associations between ultrafine/fine particle number rates and engine operating variables which complement the reported correlations in the exploratory stage of the analysis.

Tables S-1 and S-2 contain LAD regression estimates for ultrafine particle number rates. Instead of modeling the mean of particle number rates conditional on the values of the explanatory variables, tables S-1, S-2 present estimated linear models for the median. Model building was performed separately for each replication of Enfield and Farmington routes; models were based on a general to specific procedure implemented via a series of Wald tests, as reported in the paper.

Figure S-17 depicts the quadratic effects of engine speed on ultrafine particle number rates. Quadratic effects of engine speed on ultrafine particle number rates were statistically significant only in Enfield route, where the engine operated in high rpm levels. Each curve corresponds to one replication of the experiment in Enfield route.

The quantile process plots shown in figures S-18 to S-29 summarize the information that could have been presented in a series of tables like S-1, S-2, each table devoted to a single conditional quantile of ultrafine/fine particle number rates. Conditional quantiles range from 0.05 to 0.95; covariate effects that correspond to the 0.5 quantile (the median) are equal to the values reported in tables 1, 2 and S-1, S-2. Covariates are labeled as follows: Percentage Engine Load: Loadpct; Interaction between engine load and engine speed: Loadrpm; Fuel to Air Ratio: FuelAir; Fuel to Air Ratio Squared: FuelAir2; Engine Speed: EngineSpeed; Engine Speed Squared: EngineSpeed2; Boost Pressure: Boostp; Injection Pressure: Injectp; Exhaust Temperature: ExhaustT; Ambient Temperature: Temp.

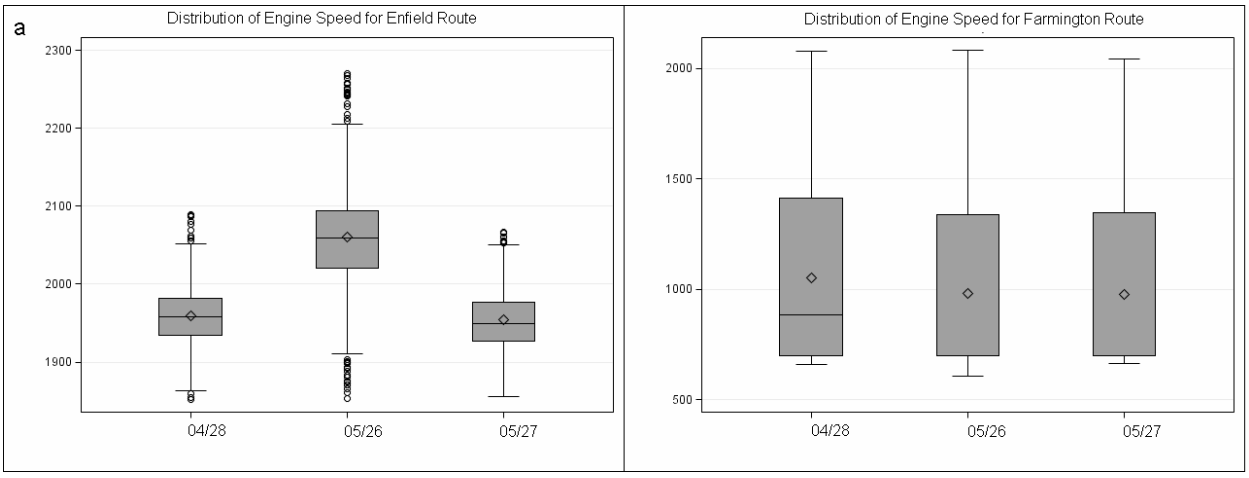

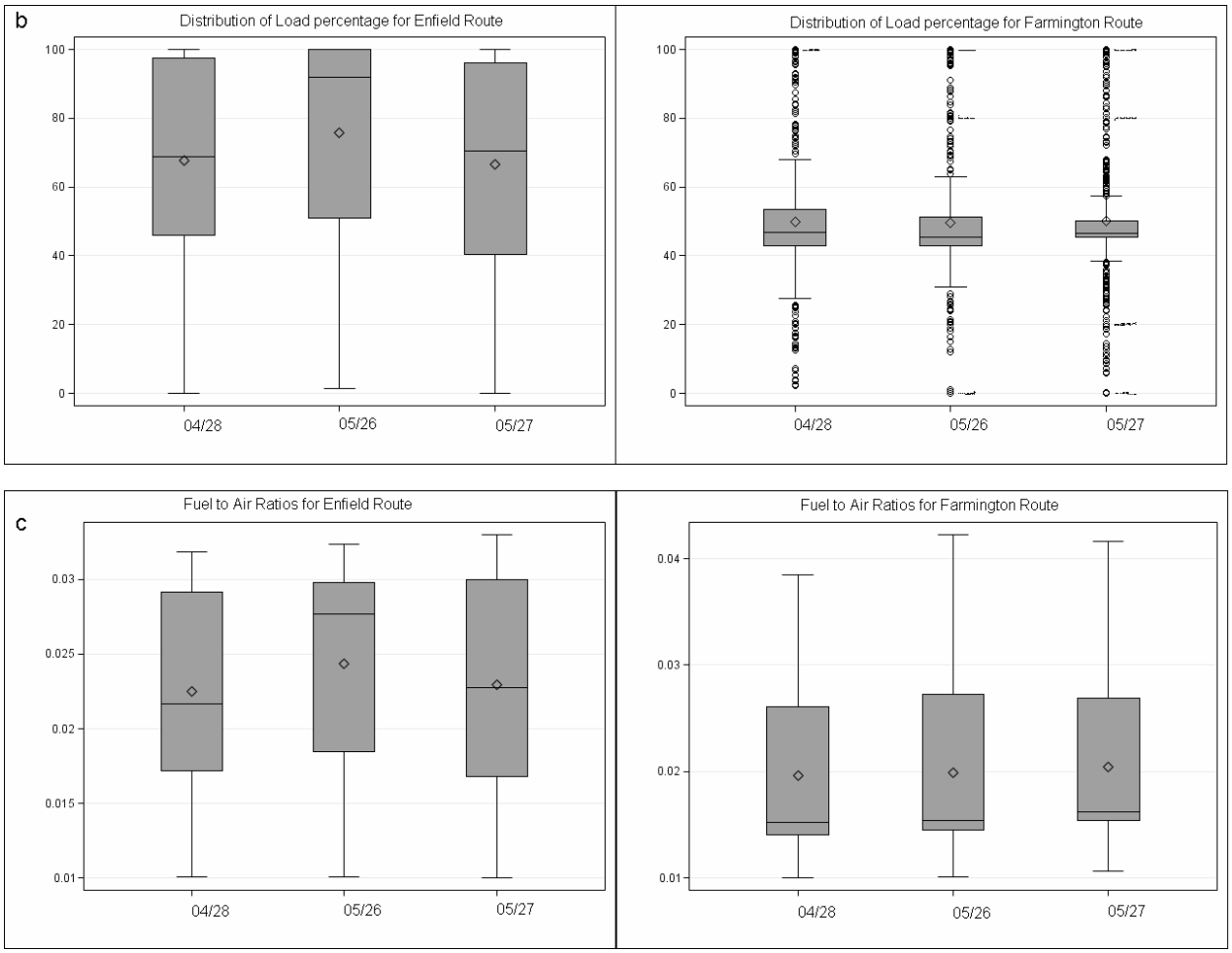


**Figure S-1. Distribution of a) engine speed (rpm) b) load percentage (%) and c) fuel to air ratio for the Enfield (left column) and Farmington routes (right column). The upper (lower) fence is defined as the third (first) quartile -represented by the upper( lower) edge of the box- plus (minus) 1.5 times the interquartile range.**

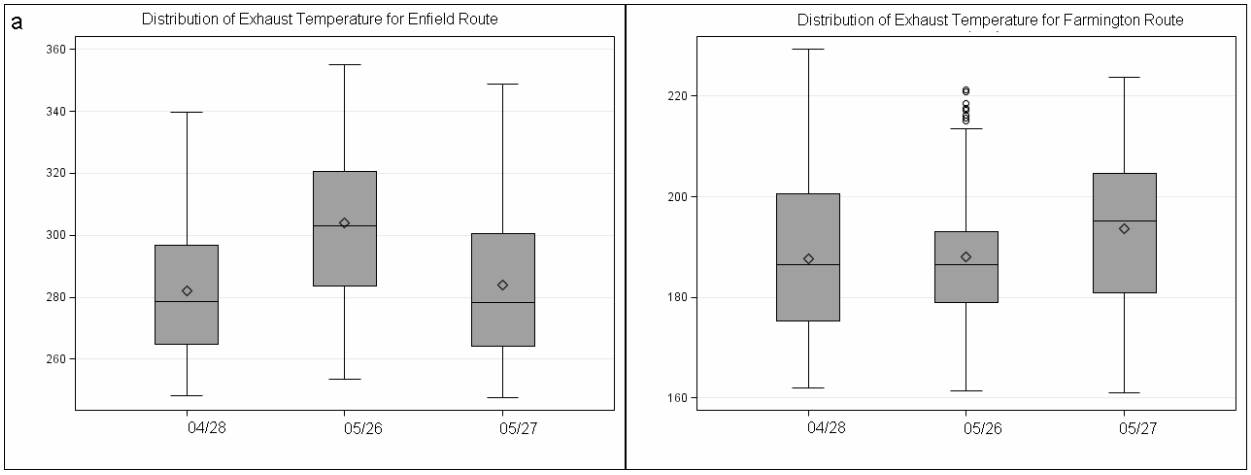

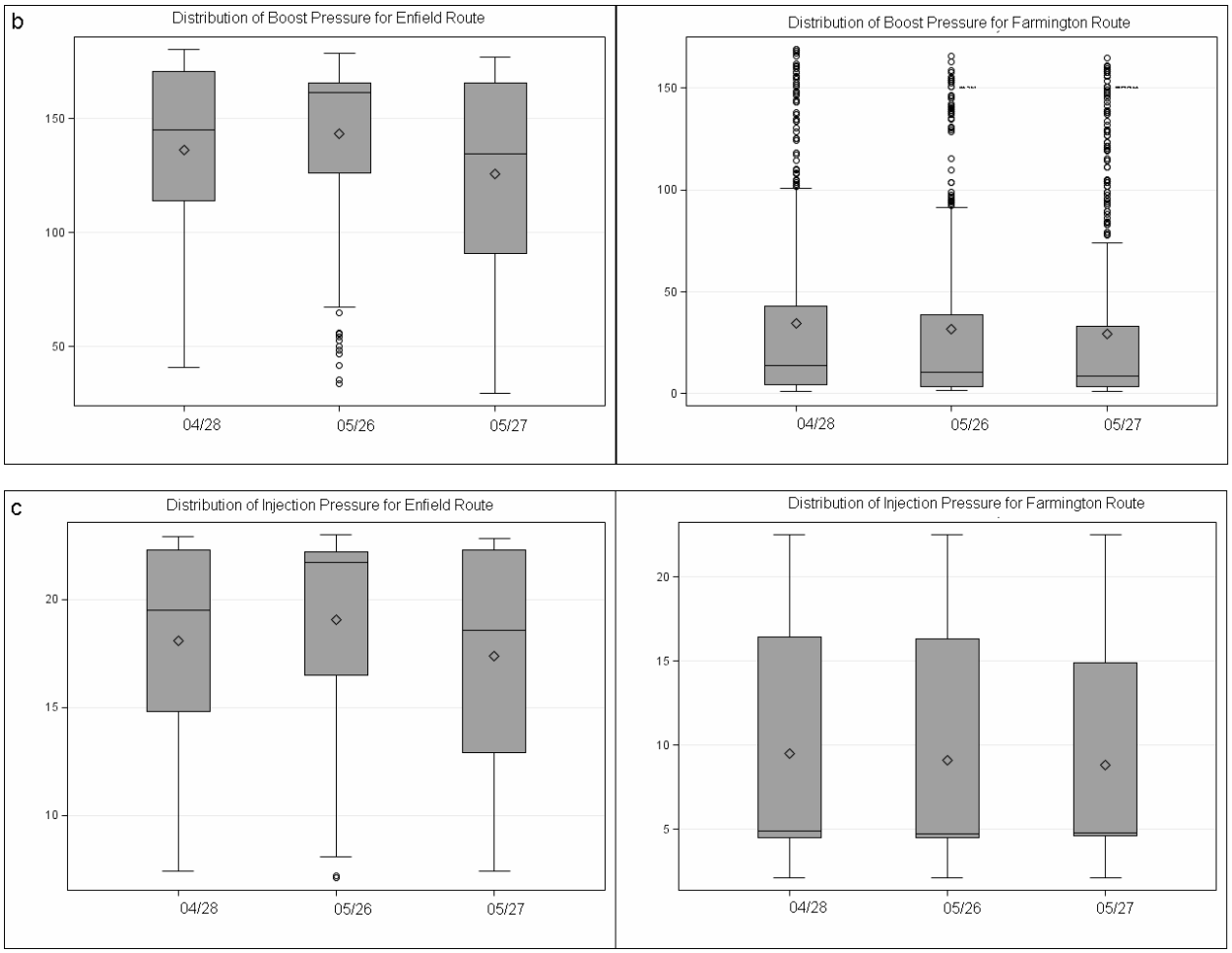


**Figure S-2. Distribution of a) exhaust temperature (K) b) boost pressure (kPa) and c) injection pressure (MPa) for the Enfield (left column) and Farmington routes (right column). The upper (lower) fence is defined as the third (first) quartile -represented by the upper( lower) edge of the box- plus (minus) 1.5 times the interquartile range.**

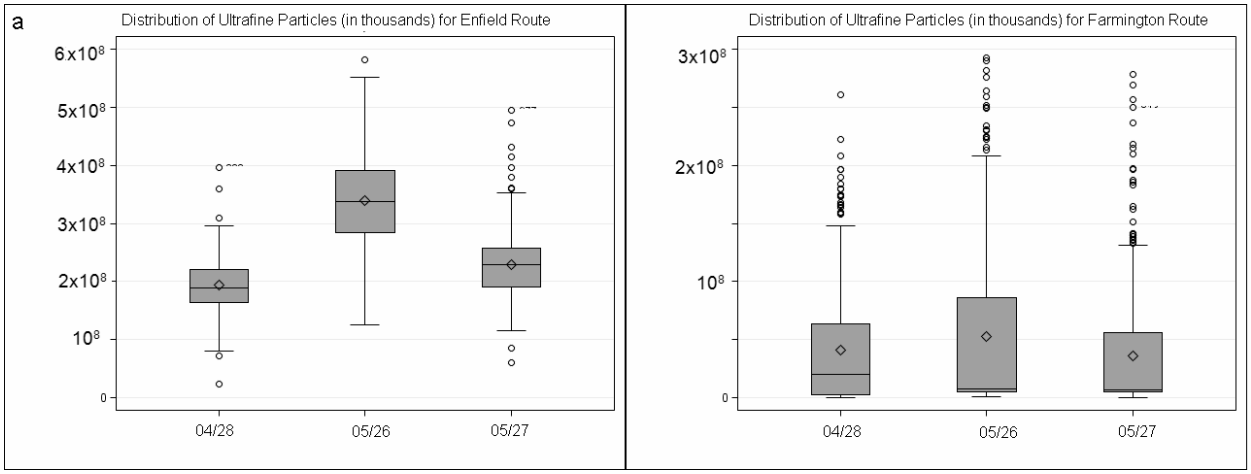

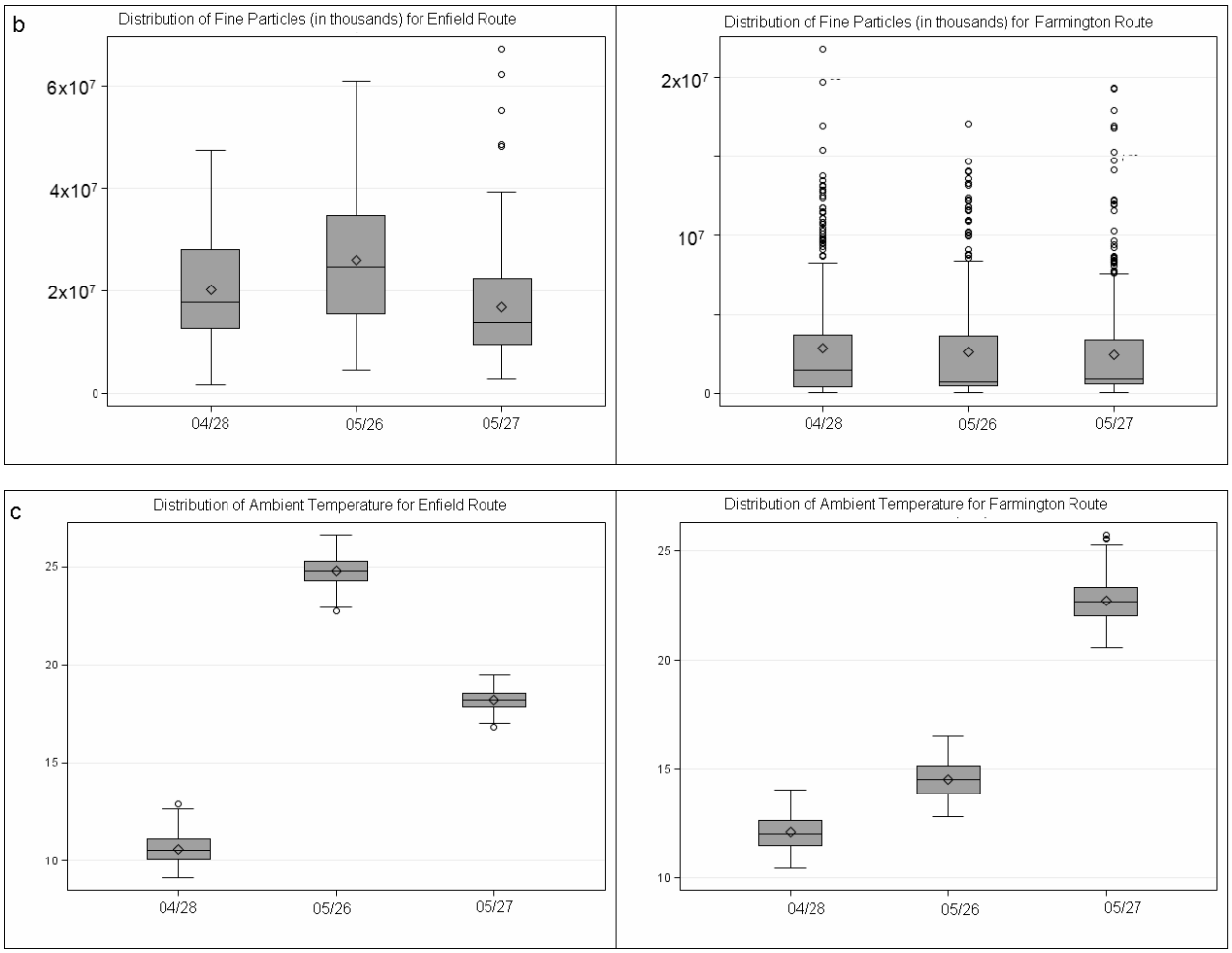


**Figure S-3. Distribution of a) ultrafine particles emission rates (in thousands per second) b) fine particles emission rates (in thousands per second) and c) ambient temperature ($^0$C) for the Enfield (left column) and Farmington routes (right column). The upper (lower) fence is defined as the third (first) quartile -represented by the upper( lower) edge of the box- plus (minus) 1.5 times the interquartile range.**

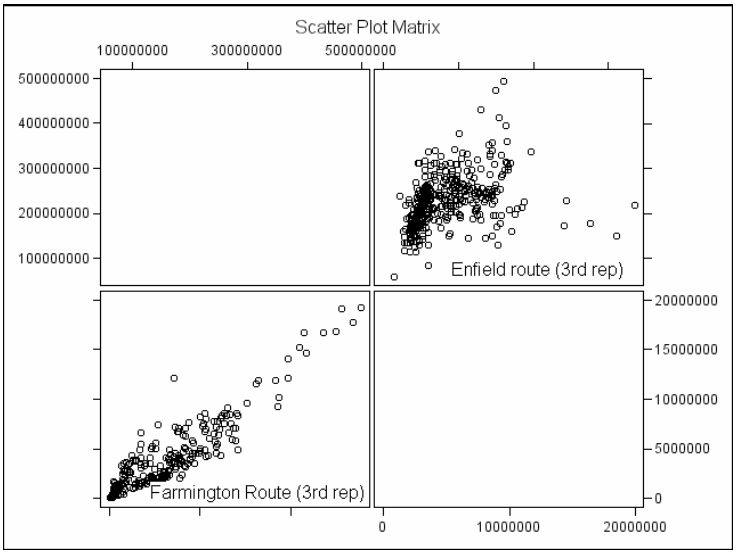

**Figure S-4. Scatter-plots for the association between ultrafine (y-axis) and fine (x-axis) emission rates in Enfield (top; the third replication is depicted) and Farmington (bottom; the third replication is depicted).**

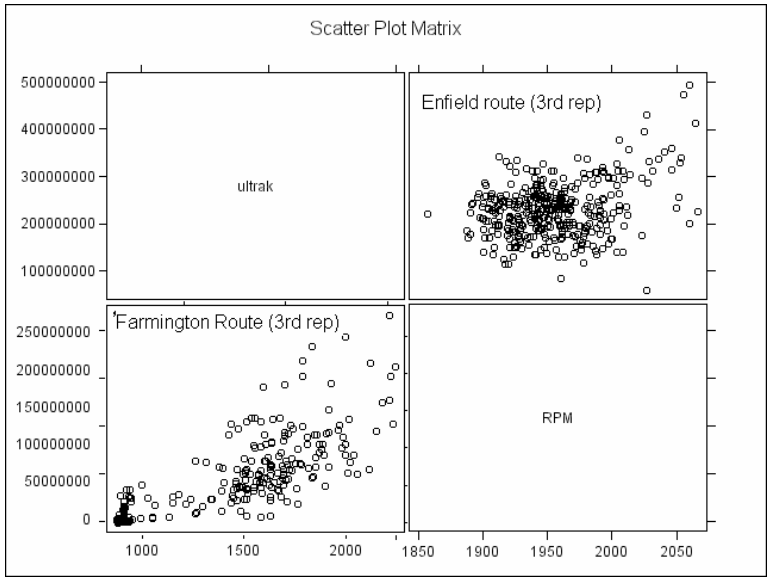


**Figure S-5. Scatter-plots for the association between ultrafine particle number rates(y-axis) and engine speed (x-axis) in Enfield (top; the third replication is depicted) and Farmington (bottom; the third replication is depicted).**

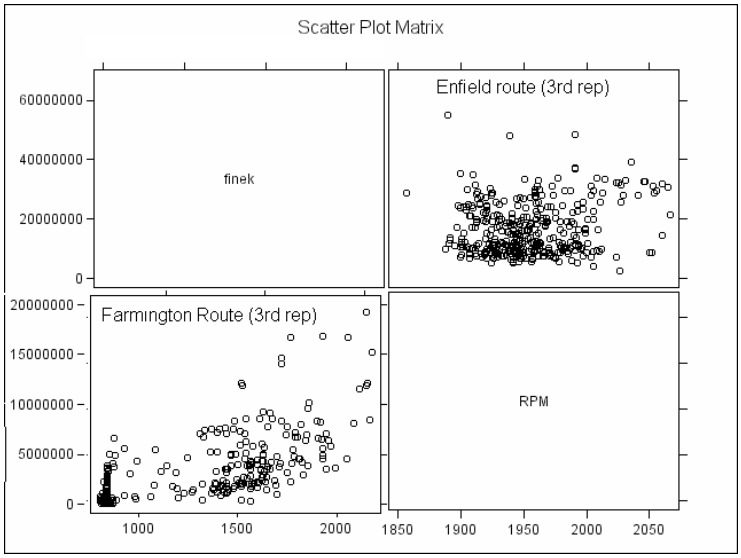


**Figure S-6. Scatter-plots for the association between fine particle number rates(y-axis) and engine speed (x-axis) in Enfield (top; the third replication is depicted) and Farmington (bottom; the third replication is depicted).**

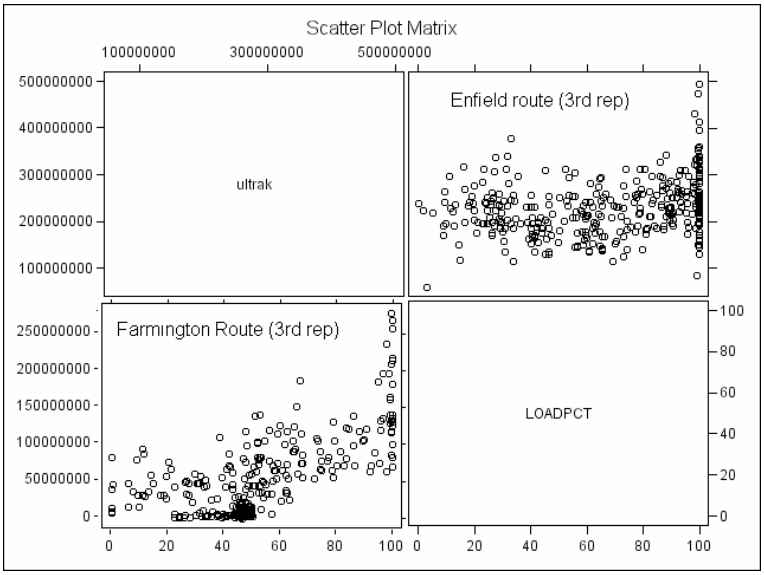


**Figure S-7. Scatter-plots for the association between ultra particle number rates(y-axis) and load engine percentage (x-axis) in Enfield (top; the third replication is depicted) and Farmington (bottom; the third replication is depicted).**

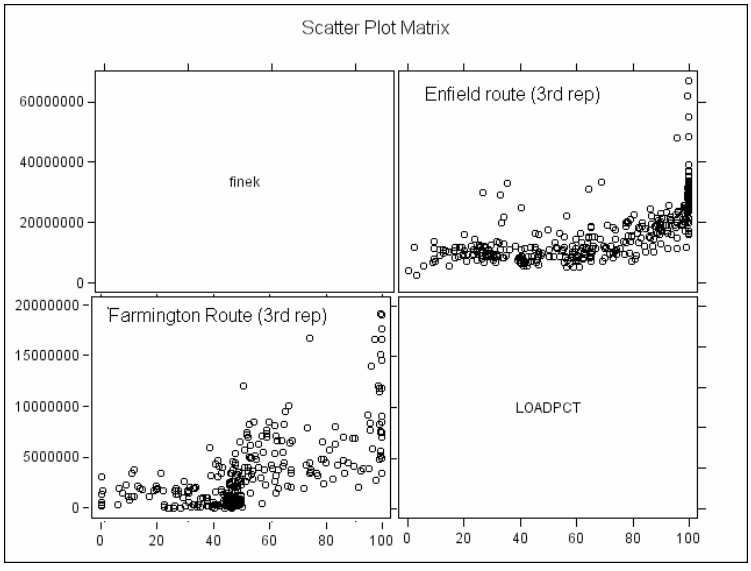


**Figure S-8. Scatter-plots for the association between fine particle number rates(y-axis) and load engine percentage (x-axis) in Enfield (top; the third replication is depicted) and Farmington (bottom; the third replication is depicted).**

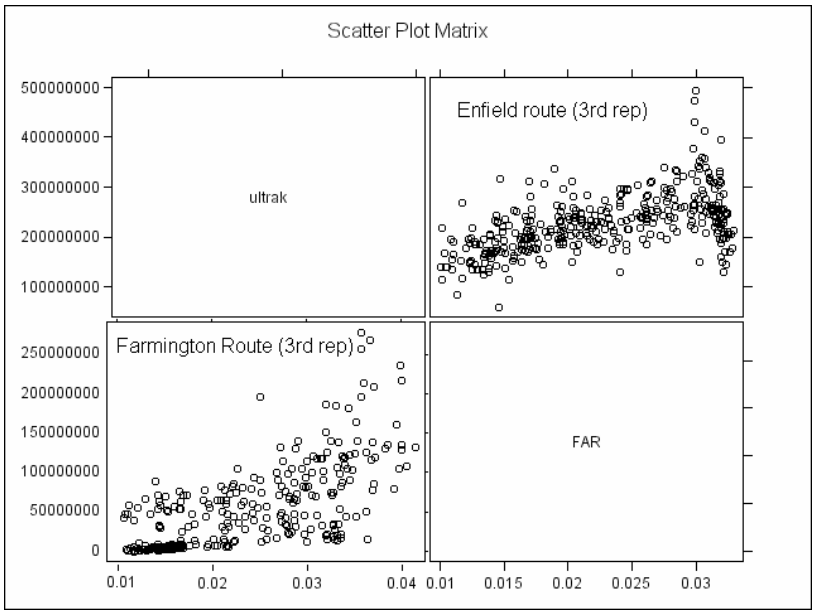


**Figure S-9. Scatter-plots for the association between ultrafine particle number rates(y-axis) and fuel to air ratios (x-axis) in Enfield (top; the third replication is depicted) and Farmington (bottom; the third replication is depicted).**

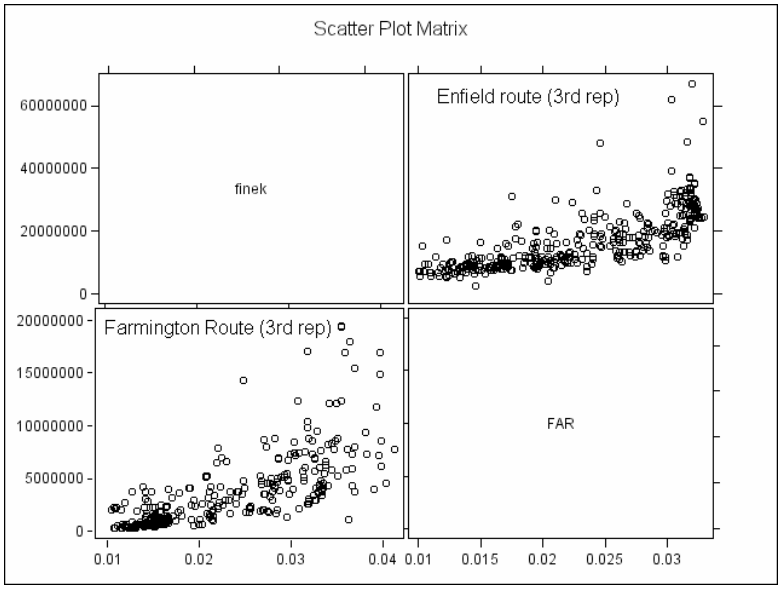


**Figure S-10. Scatter-plots for the association between fine particle number rates (y-axis) and fuel to air ratios (x-axis) in Enfield (top; the third replication is depicted) and Farmington (bottom; the third replication is depicted).**

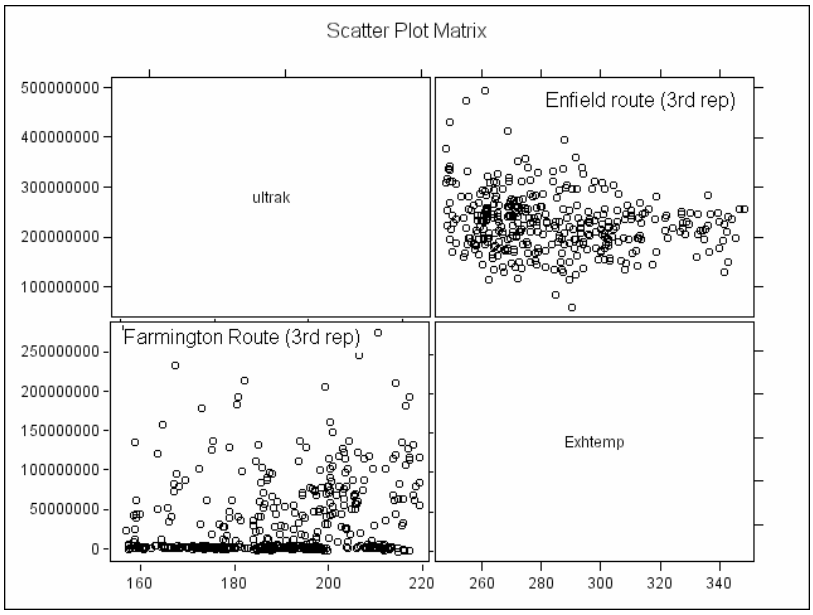


**Figure S-11. Scatter-plots for the association between ultrafine particle number rates(y-axis) and exhaust temperature (x-axis) in Enfield (top; the third replication is depicted) and Farmington (bottom; the third replication is depicted).**

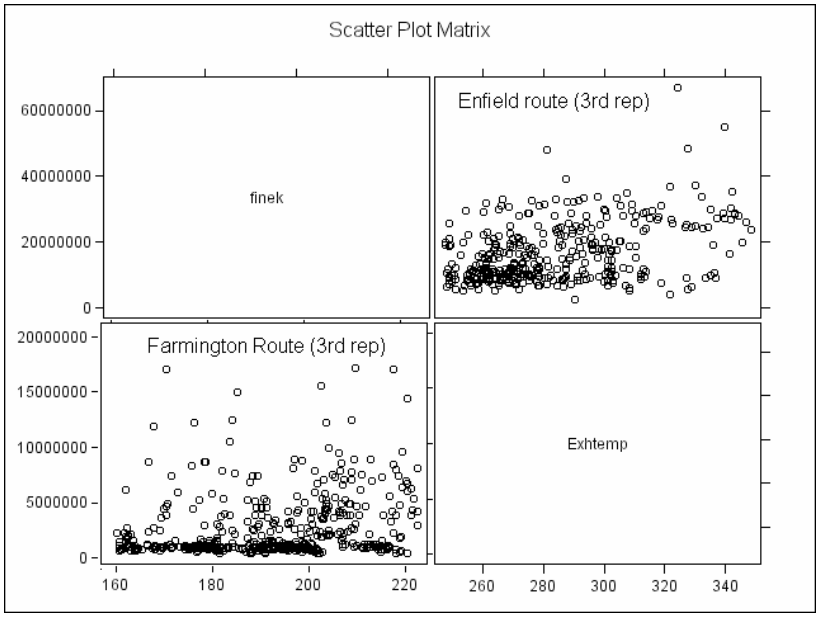


**Figure S-12. Scatter-plots for the association between fine particle number rates(y-axis) and exhaust temperature (x-axis) in Enfield (top; the third replication is depicted) and Farmington (bottom; the third replication is depicted).**

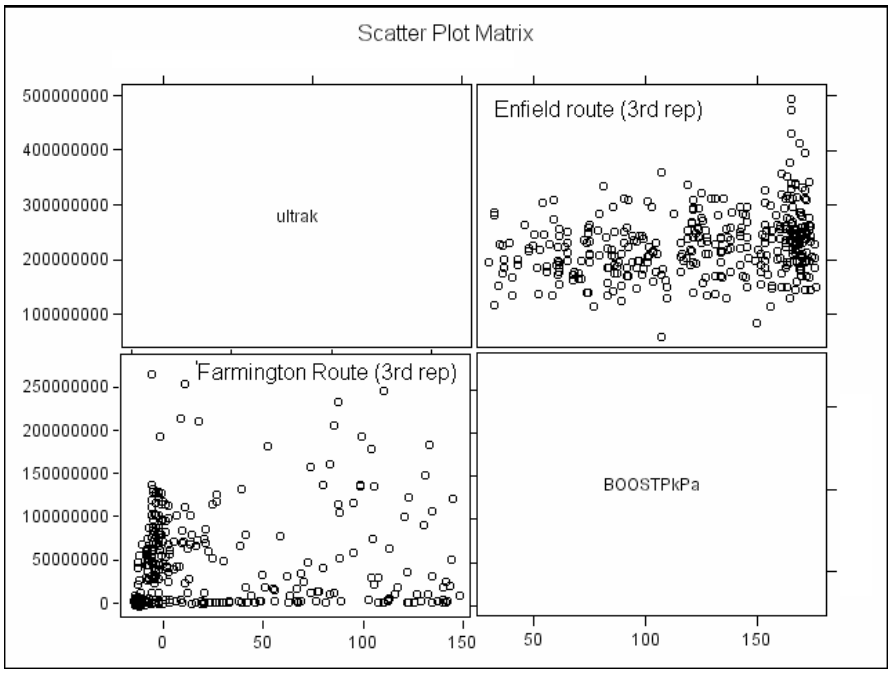


**Figure S-13. Scatter-plots for the association between ultrafine particle number rates(y-axis) and boost pressure (x-axis) in Enfield (top; the third replication is depicted) and Farmington (bottom; the third replication is depicted).**

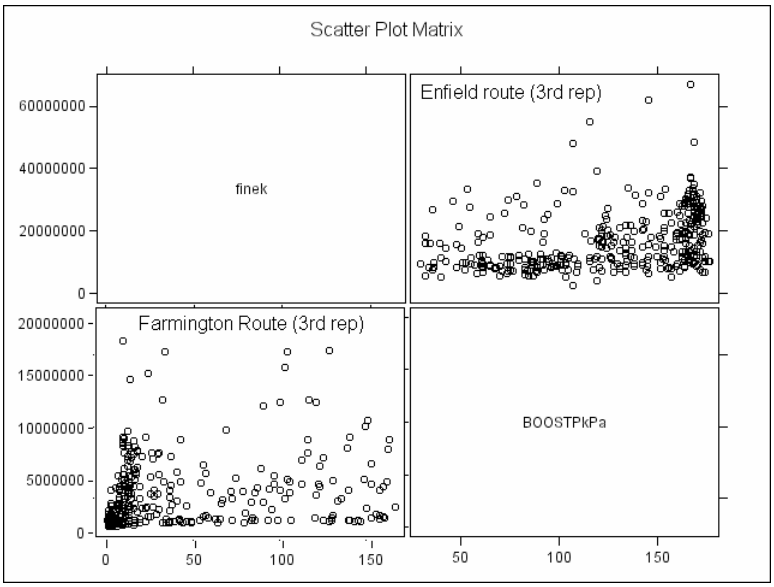


**Figure S-14. Scatter-plots for the association between fine particle number rates(y-axis) and boost pressure (x-axis) in Enfield (top; the third replication is depicted) and Farmington (bottom; the third replication is depicted).**

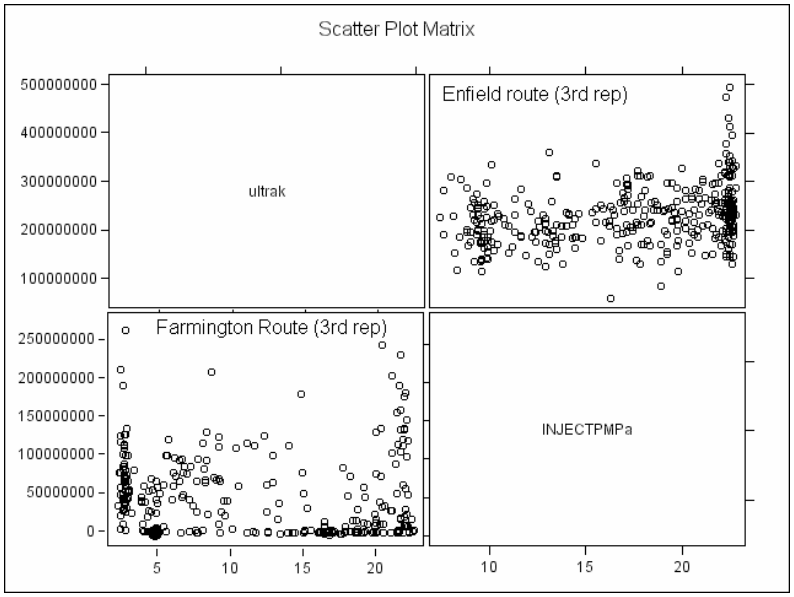


**Figure S-15. Scatter-plots for the association between ultrafine particle number rates(y-axis) and injection pressure (x-axis) in Enfield (top; the third replication is depicted) and Farmington (bottom; the third replication is depicted).**

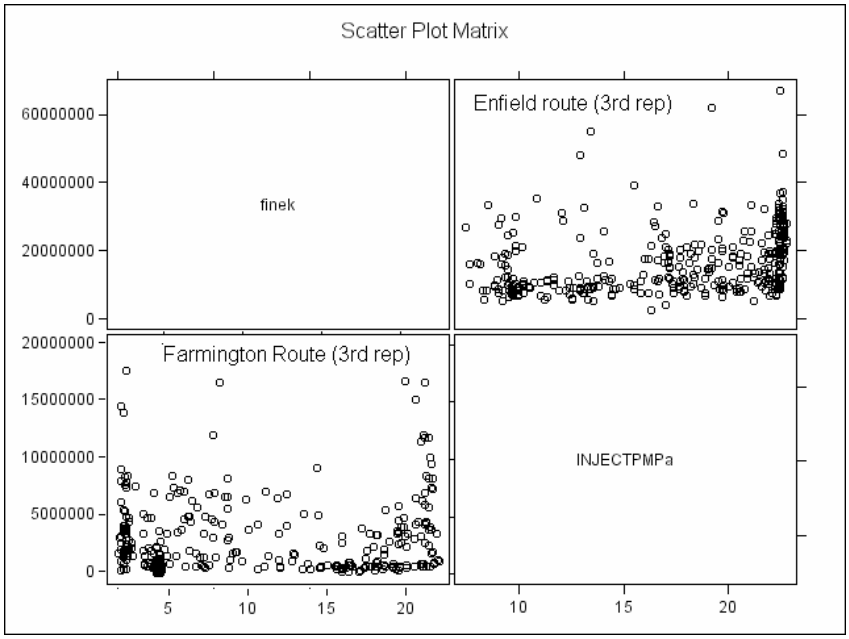


**Figure S-16. Scatter-plots for the association between fine particle number rates(y-axis) and injection pressure (x-axis) in Enfield (top; the third replication is depicted) and Farmington (bottom; the third replication is depicted).**

**Table S-1. LAD regression estimates, 95% confidence limits based on the heteroscedasticity robust resampling method of He and Hu (2002), t-statistics and corresponding p-values, for the effects of engine operating variables on the square root of ultrafine particle number emission rates observed in Enfield route. The general-to-specific model building procedure was adopted, based on a series of Wald tests. The three replications of the experiment correspond to the following days (from top): 04/28/2004, 05/26/2004 and 05/27/2004.**

| *Parameter* | *Estimate* | *Stand. Error* | *95% Conf.* | *Limits* | *t Value* | *Pr > \|t\|* |
|---|---|---|---|---|---|---|
| *Intercept* | 14195.52 | 941.5504 | 12344.18 | 16046.85 | 15.08 | <.0001 |
| *loadpct* | -217.411 | 26.7882 | -270.083 | -164.738 | -8.12 | <.0001 |
| *Load*rpm* | 0.1602 | 0.0199 | 0.1211 | 0.1994 | 8.05 | <.0001 |
| *FuelAir* | 537975 | 59842.84 | 420308.4 | 655641.5 | 8.99 | <.0001 |
| *FuelAir^2* | -1.12E+07 | 1703256 | -1.46E+07 | -7863603 | -6.58 | <.0001 |
| *ExhaustTemp* | -25.0962 | 3.1375 | -31.2654 | -18.9271 | -8 | <.0001 |
| *Amb.Temp* | 167.7028 | 79.1267 | 12.1192 | 323.2865 | 2.12 | 0.035 |
| *Intercept* | 17484.41 | 1041.485 | 15436.76 | 19532.05 | 16.79 | <.0001 |
| *loadpct* | -267.927 | 17.1042 | -301.555 | -234.299 | -15.66 | <.0001 |
| *Load*rpm* | 0.1909 | 0.0106 | 0.1701 | 0.2118 | 17.99 | <.0001 |
| *FuelAir* | 157666.1 | 12941.25 | 132222.5 | 183109.6 | 12.18 | <.0001 |
| *ExhaustTemp* | -13.9444 | 3.7412 | -21.2998 | -6.5889 | -3.73 | 0.0002 |
| *Amb. Temp.* | 0.2561 | 120.6459 | -236.943 | 237.4556 | 0 | 0.998 |

| | | | | | | |
|---|---|---|---|---|---|---|
| *Intercept* | 15966.38 | 1218.558 | 13570.06 | 18362.7 | 13.1 | <.0001 |
| *loadpct* | -230.959 | 37.6326 | -304.964 | -156.954 | -6.14 | <.0001 |
| *Load*rpm* | 0.1678 | 0.0274 | 0.1139 | 0.2218 | 6.12 | <.0001 |
| *FuelAir* | 367734.6 | 77098.17 | 216119.4 | 519349.7 | 4.77 | <.0001 |
| *ExhaustTemp* | -4765954 | 2171917 | -9037074 | -494834 | -2.19 | 0.0288 |
| *Amb. Temp.* | -26.9465 | 4.6652 | -36.1206 | -17.7724 | -5.78 | <.0001 |

**Table S-2. LAD regression estimates, 95% confidence limits based on the heteroscedasticity robust resampling method of He and Hu (2002), t-statistics and corresponding p-values, for the effects of engine operating variables on the square root of ultrafine particle number emission rates observed in Farmington route. The general-to-specific model building procedure was adopted, based on a series of Wald tests. The three replications of the experiment correspond to the following days (from top): 04/28/2004, 05/26/2004 and 05/27/2004.**

| *Parameter* | *Estimate* | *Stand. Error* | *95% Conf.* | *Limits* | *t Value* | *Pr > \|t\|* |
|---|---|---|---|---|---|---|
| *Load*rpm* | 0.0479 | 0.0088 | 0.0251 | 0.0706 | 5.44 | <.0001 |
| *EngineSpeed* | 9.957 | 0.6478 | 8.2796 | 11.6343 | 15.37 | <.0001 |
| *EngineSpeed^2* | -0.0049 | 0.0008 | -0.0071 | -0.0027 | -5.82 | <.0001 |
| *FuelAir* | 75657.08 | 14642.49 | 37745.55 | 113568.6 | 5.17 | <.0001 |
| *Boostp* | 5.1563 | 1.4032 | 1.5233 | 8.7893 | 3.67 | 0.0003 |
| *Amb.Temp* | 48.5178 | 29.8675 | -28.8136 | 125.8492 | 1.62 | 0.1051 |
| *Load*rpm* | 0.0576 | 0.009 | 0.0342 | 0.081 | 6.38 | <.0001 |
| *EngineSpeed* | 11.6177 | 0.7818 | 9.5932 | 13.6423 | 14.86 | <.0001 |
| *EngineSpeed^2* | -0.0063 | 0.0008 | -0.0082 | -0.0043 | -8.23 | <.0001 |
| *FuelAir* | 132142.7 | 9666.751 | 107110.1 | 157175.3 | 13.67 | <.0001 |
| *Amb.Temp* | 130.2251 | 47.1401 | 8.1532 | 252.297 | 2.76 | 0.006 |
| *Load*rpm* | 0.0454 | 0.007 | 0.0273 | 0.0635 | 6.49 | <.0001 |
| *EngineSpeed* | 8.8373 | 0.6511 | 7.1533 | 10.5213 | 13.57 | <.0001 |
| *EngineSpeed^2* | -0.0051 | 0.0007 | -0.0068 | -0.0033 | -7.5 | <.0001 |

| | | | | | | |
|---|---|---|---|---|---|---|
| *FuelAir* | 133310.9 | 12084.22 | 102058.2 | 164563.6 | 11.03 | <.0001 |
| *Amb.Temp* | -7.4232 | 17.3483 | -52.2903 | 37.4438 | -0.43 | 0.6689 |

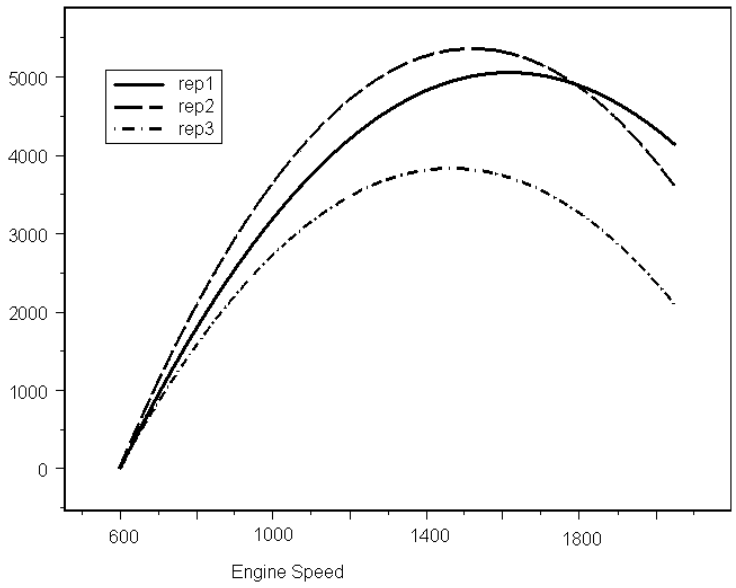


**Figure S-17. Estimated engine-speed (rpm) effects at the median of the conditional distribution of ultrafine particle number emission rates for three replications of Farmington route.**

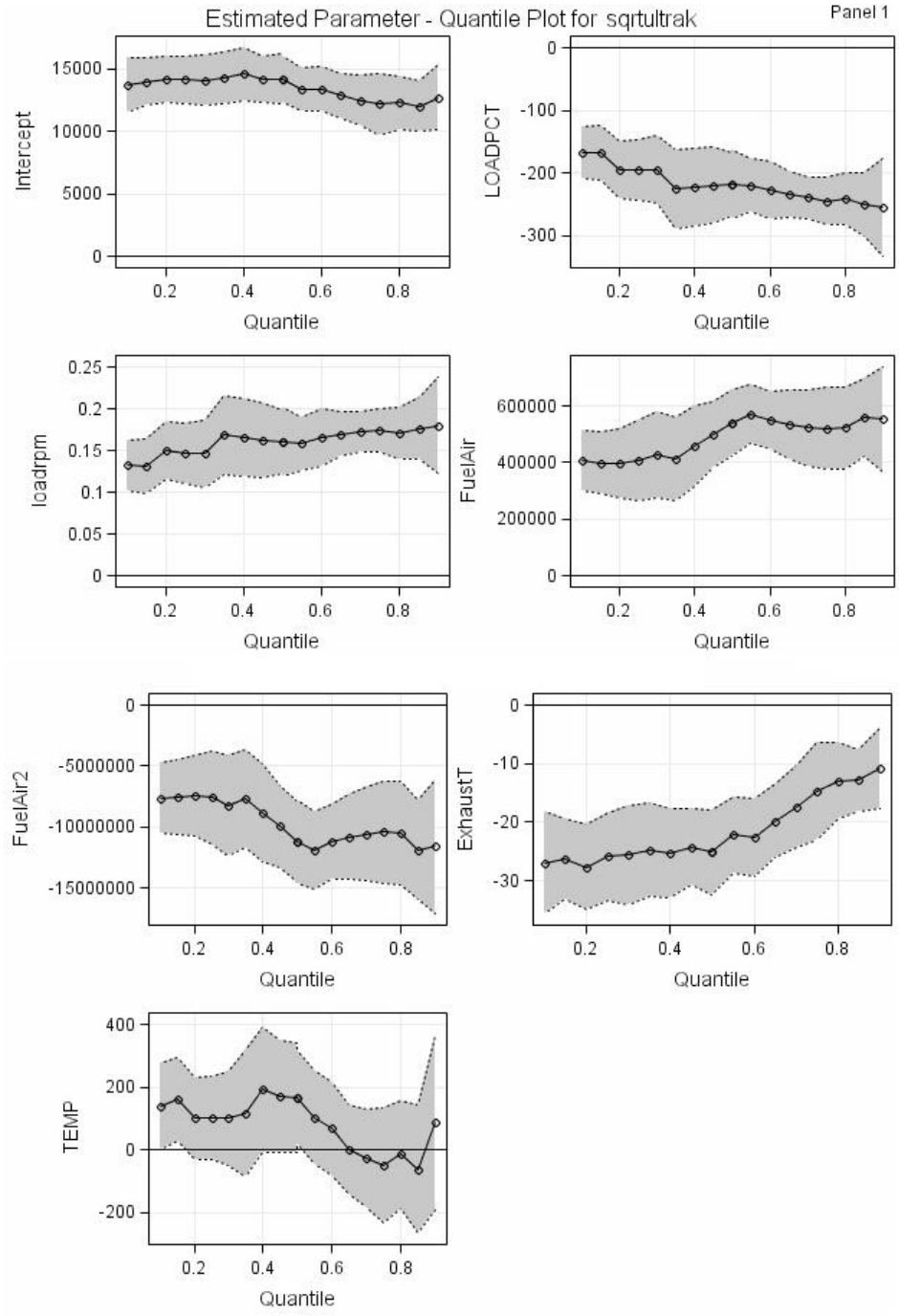


**Figure S-18. Quantile regression process plots for the covariate effects on (the square root of) ultrafine particle number rates. The figures correspond to the first replication of the experiment in Enfield. A 95% point-wise confidence band for the quantile regression parameters is indicated by the shaded region. The solid horizontal line indicates the null effect.**

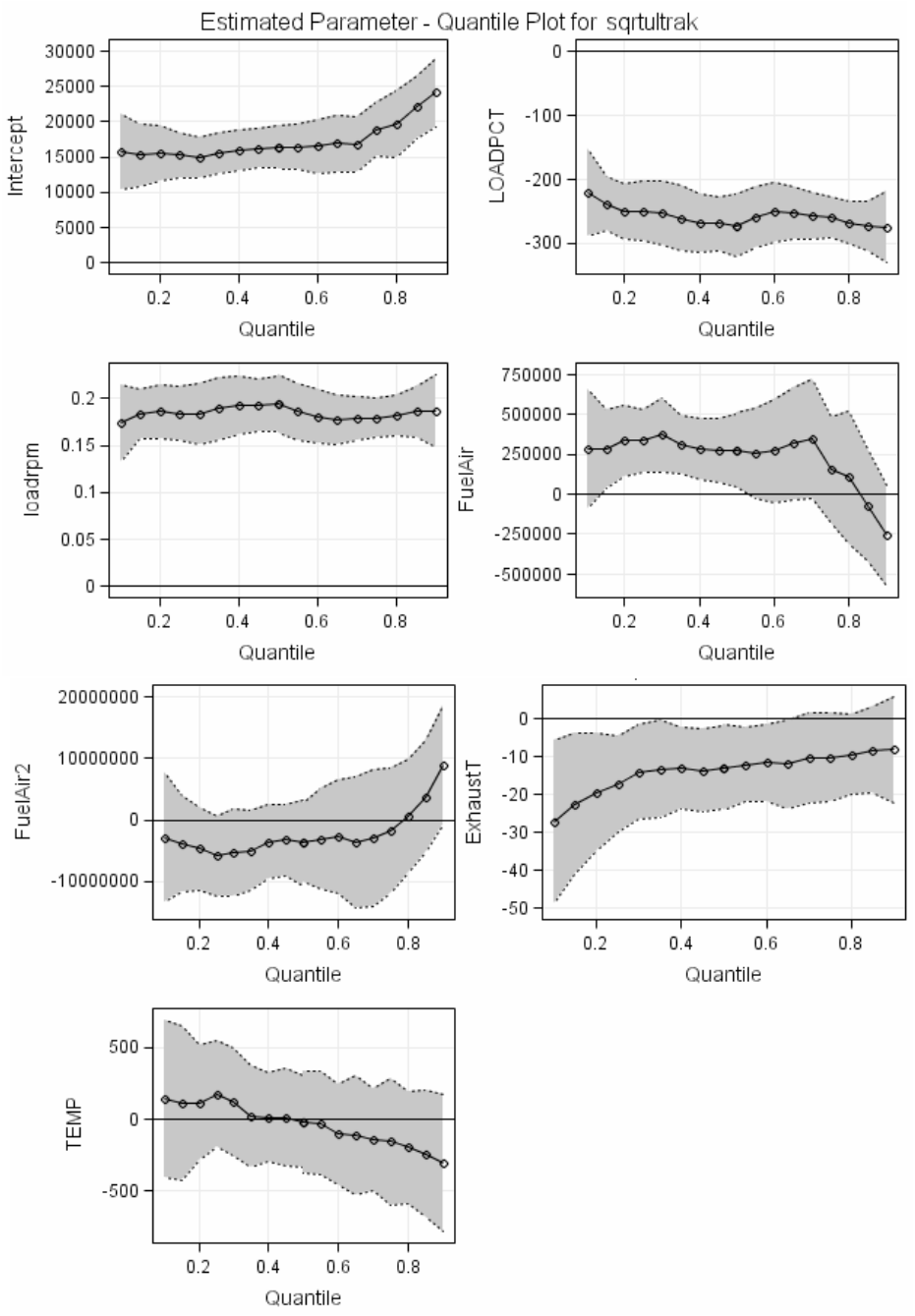


**Figure S-19. Quantile regression process plots for covariate effects on (the square root of) ultrafine particle number rates. The figures correspond to the second replication of the experiment in Enfield. A 95% point-wise confidence band for the quantile regression parameters is indicated by the shaded region. The solid horizontal line indicates the null effect.**

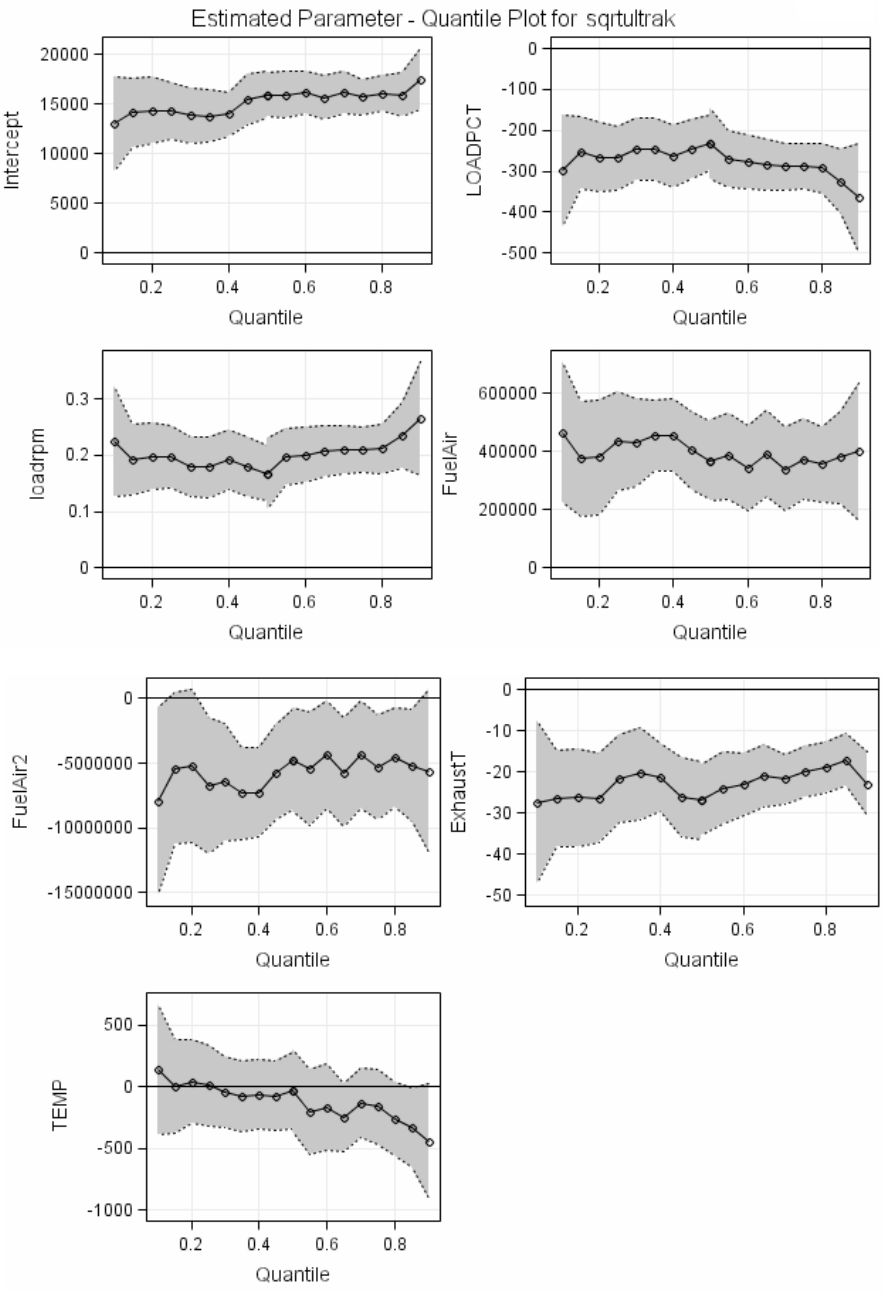


**Figure S-20. Quantile regression process plots for covariate effects on (the square root of) ultrafine particle number rates. The figures correspond to the third replication of the experiment in Enfield. A 95% point-wise confidence band for the quantile regression parameters is indicated by the shaded region. The solid horizontal line indicates the null effect.**

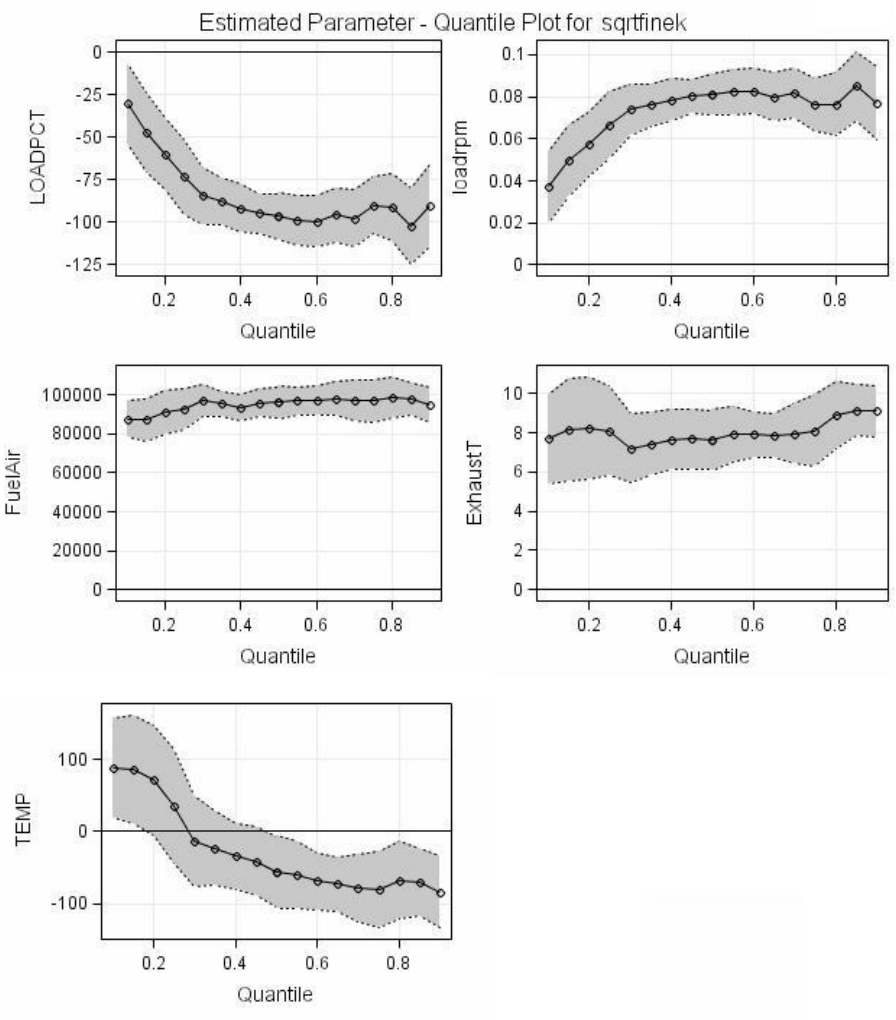


**Figure S-21. Quantile regression process plots for covariate effects on (the square root of) fine particle number rates. The figure corresponds to the first replication of the experiment in Enfield route. A 95% point-wise confidence band for the quantile regression parameters is indicated by the shaded region. The solid horizontal line indicates the null effect.**

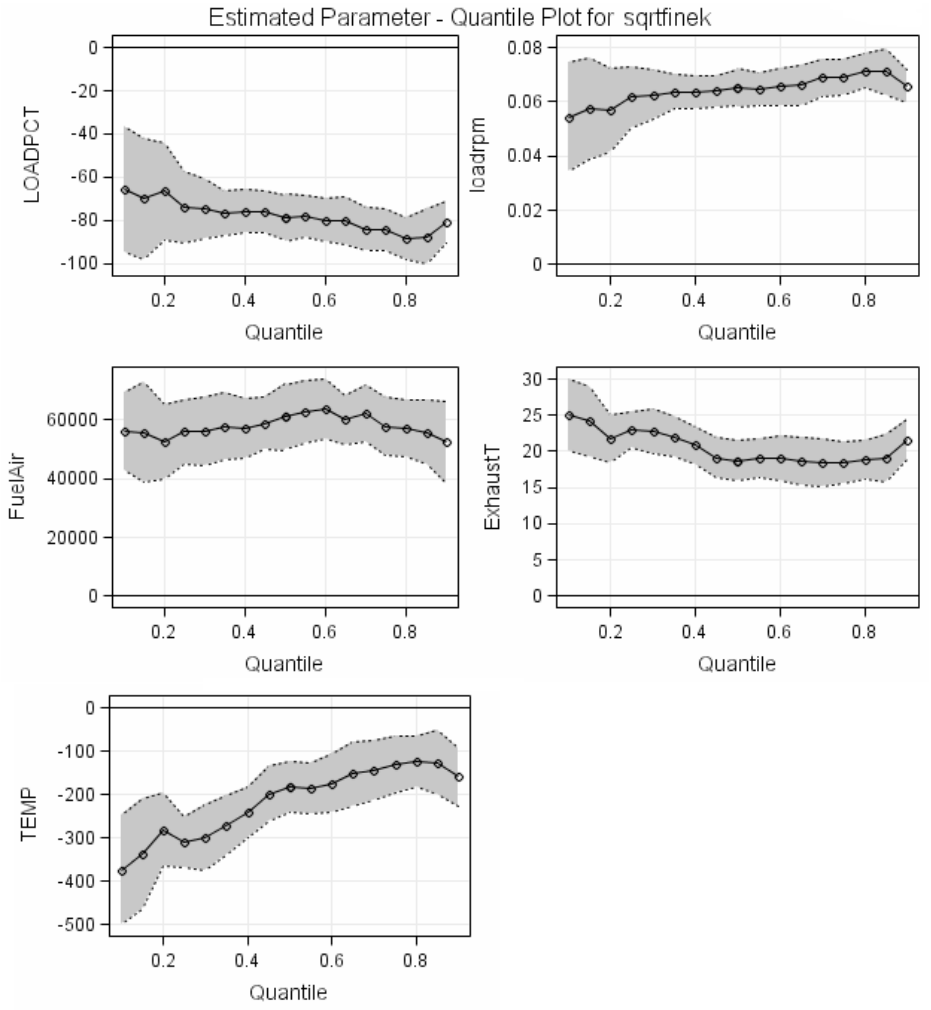


**Figure S-22. Quantile regression process plots for covariate effects on (the square root of) fine particle number rates. The figure corresponds to the second replication of the experiment in Enfield route. A 95% point-wise confidence band for the quantile regression parameters is indicated by the shaded region. The solid horizontal line indicates the null effect.**

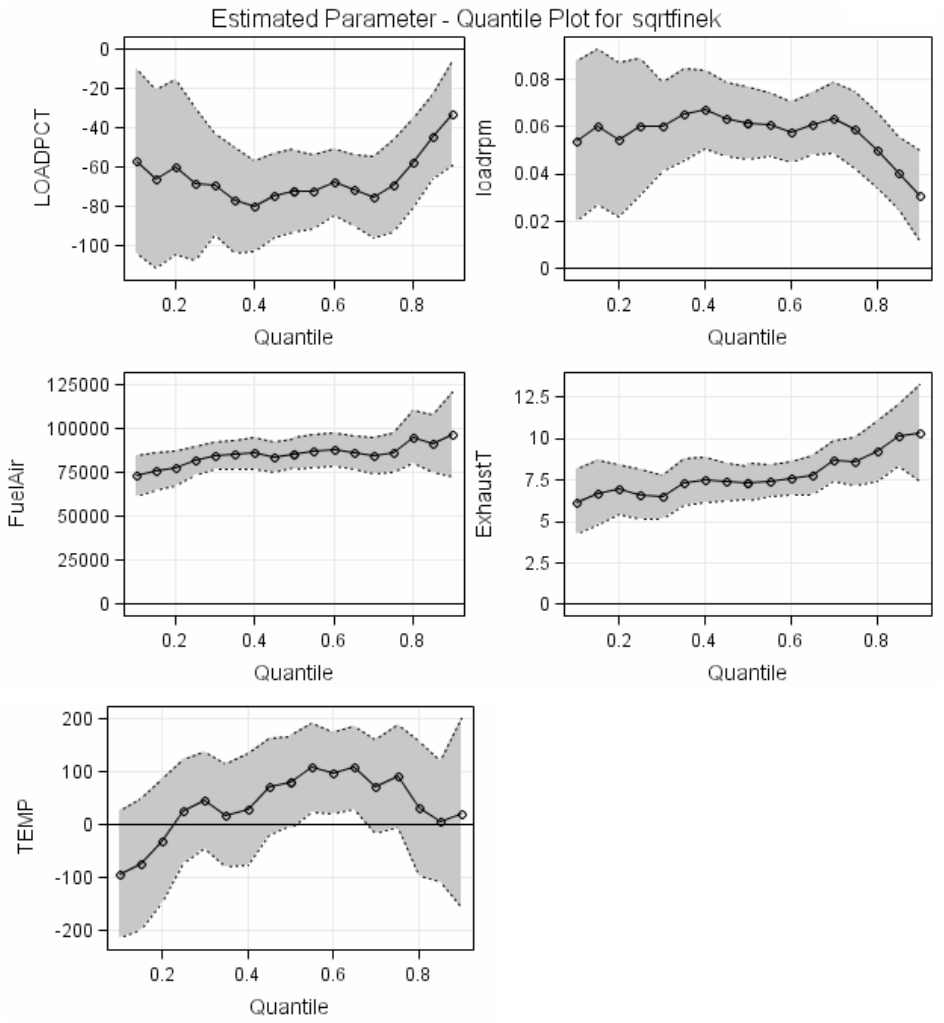


**Figure S-23. Quantile regression process plots for covariate effects on (the square root of) fine particle number rates. The figure corresponds to the third replication of the experiment in Enfield route. A 95% point-wise confidence band for the quantile regression parameters is indicated by the shaded region. The solid horizontal line indicates the null effect.**

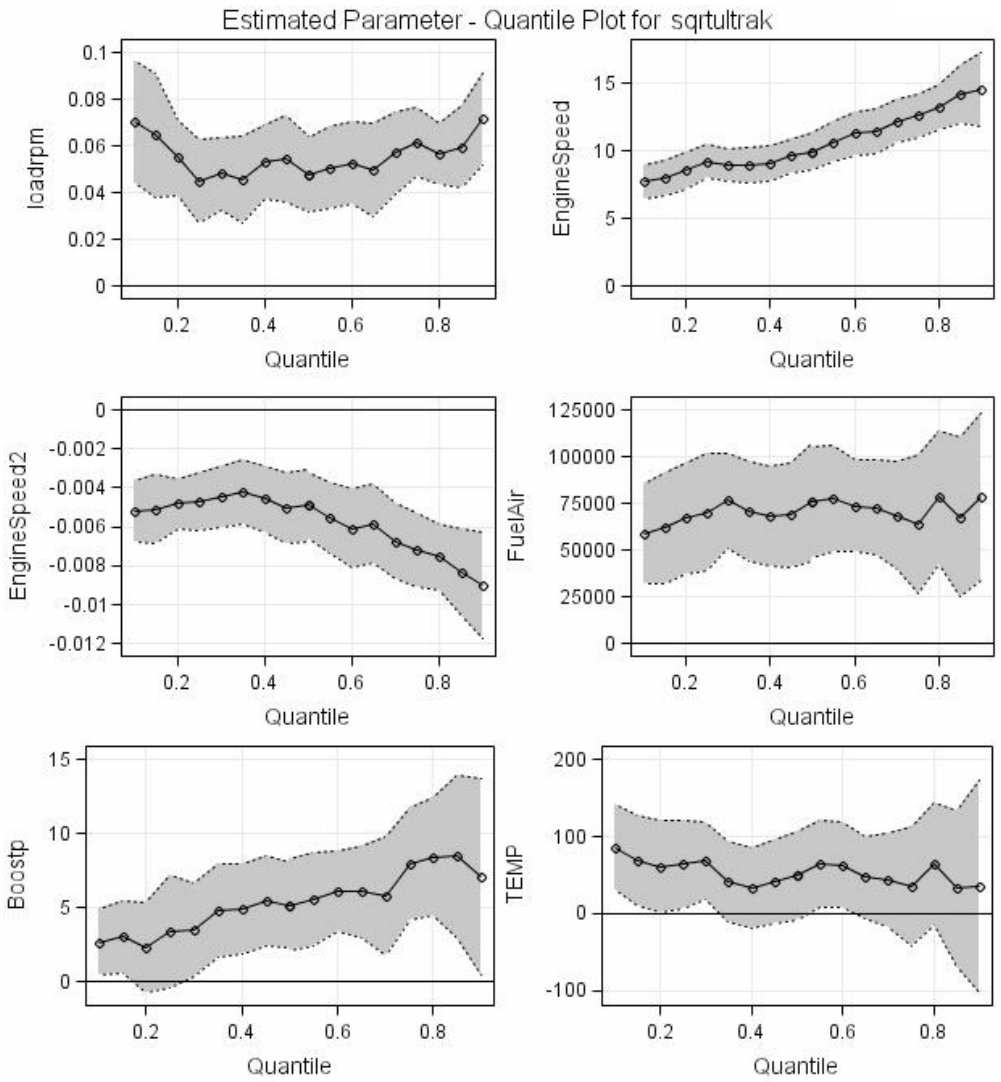


**Figure S-24. Quantile regression process plots for covariate effects on (the square root of) ultrafine particle number rates. The figure corresponds to the first replication of the experiment in Farmington route. A 95% point-wise confidence band for the quantile regression parameters is indicated by the shaded region. The solid horizontal line indicates the null effect.**

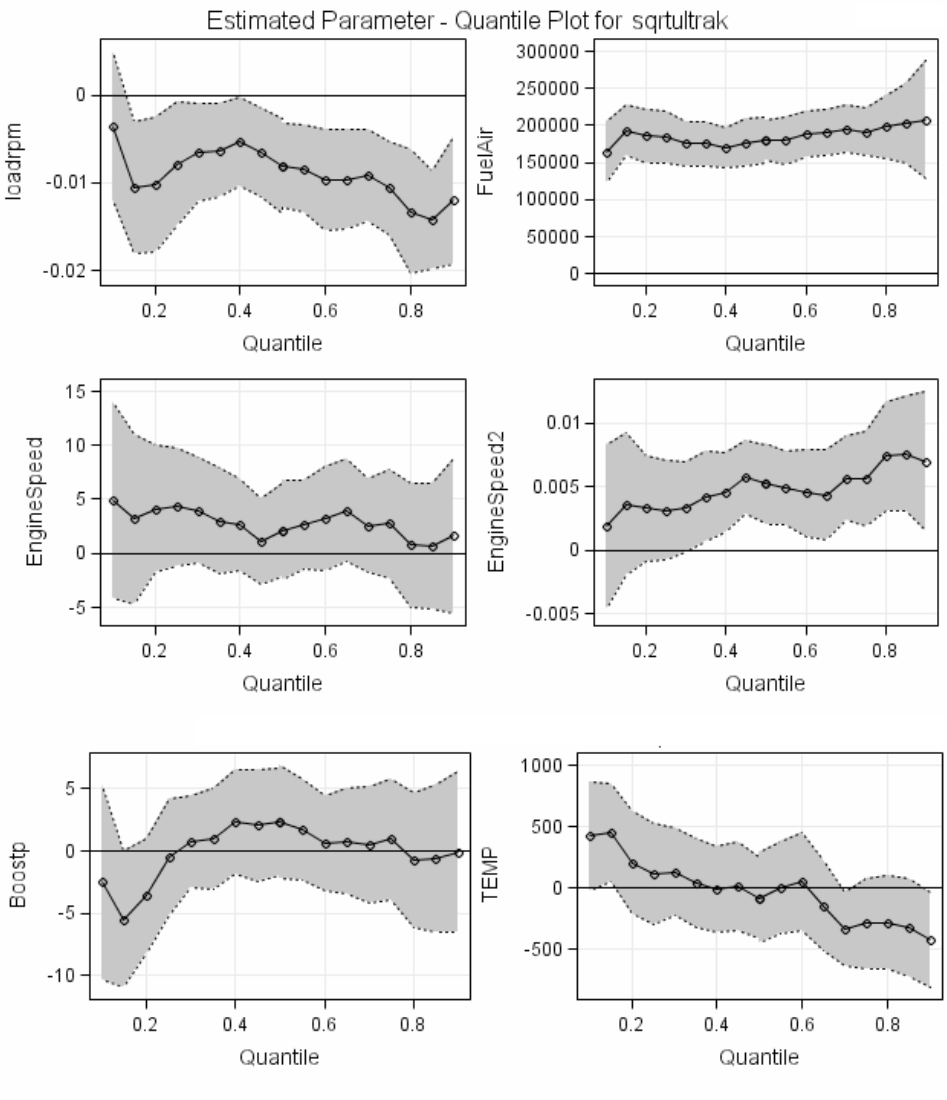


**Figure S-25. Quantile regression process plots for covariate effects on (the square root of) ultrafine particle number rates. The figure corresponds to the second replication of the experiment in Farmington route. A 95% point-wise confidence band for the quantile regression parameters is indicated by the shaded region. The solid horizontal line indicates the null effect.**

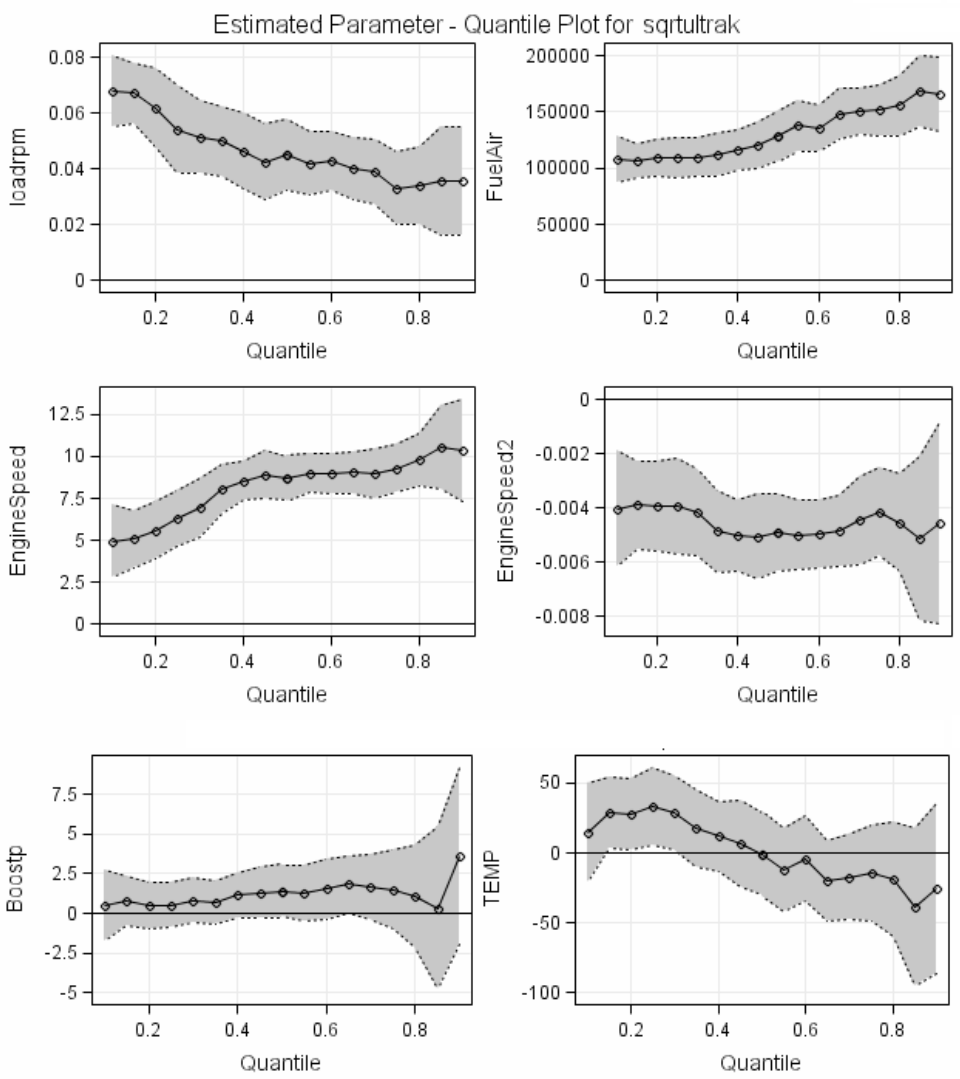


**Figure S-26. Quantile regression process plots for covariate effects on (the square root of) ultrafine particle number rates. The figure corresponds to the third replication of the experiment in Farmington route. A 95% point-wise confidence band for the quantile regression parameters is indicated by the shaded region. The solid horizontal line indicates the null effect.**

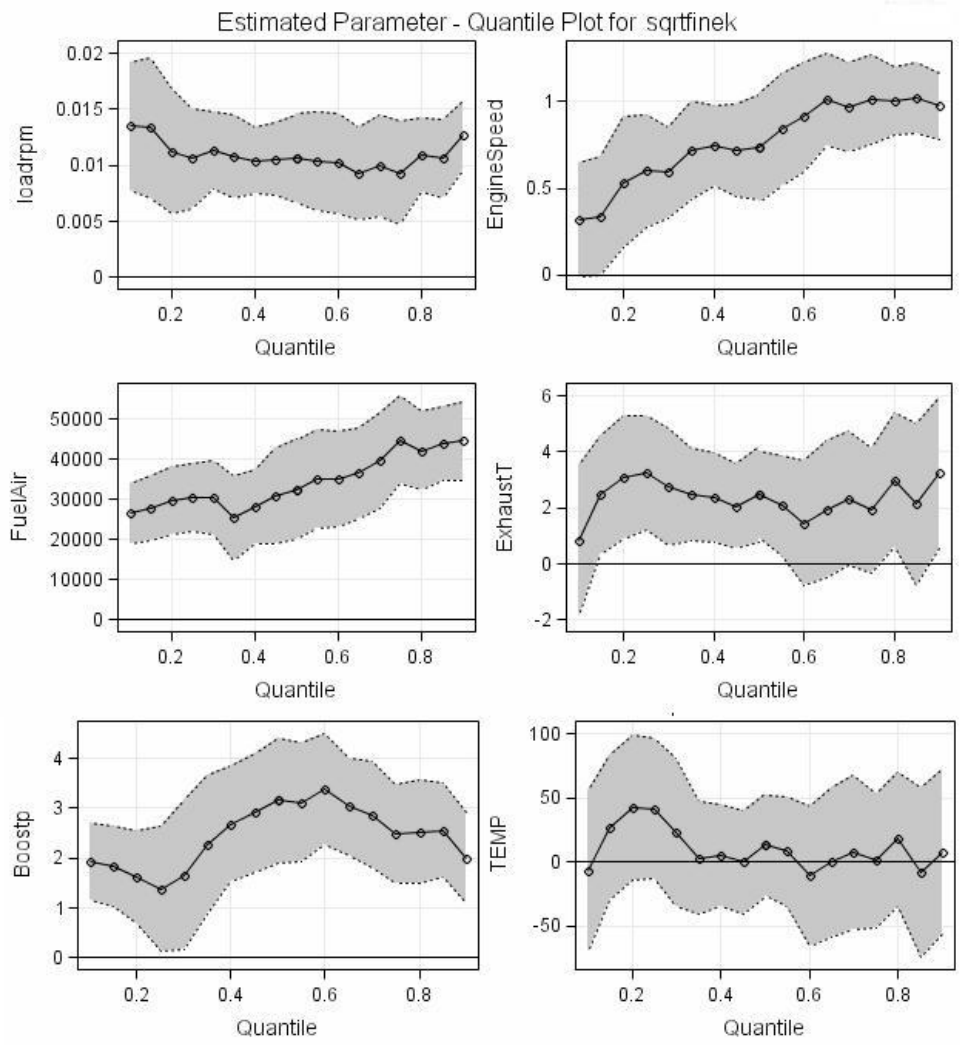


**Figure S-27. Quantile regression process plots for covariate effects on (the square root of) fine particle number rates. The figure corresponds to the first replication of the experiment in Farmington route. A 95% point-wise confidence band for the quantile regression parameters is indicated by the shaded region. The solid horizontal line indicates the null effect.**

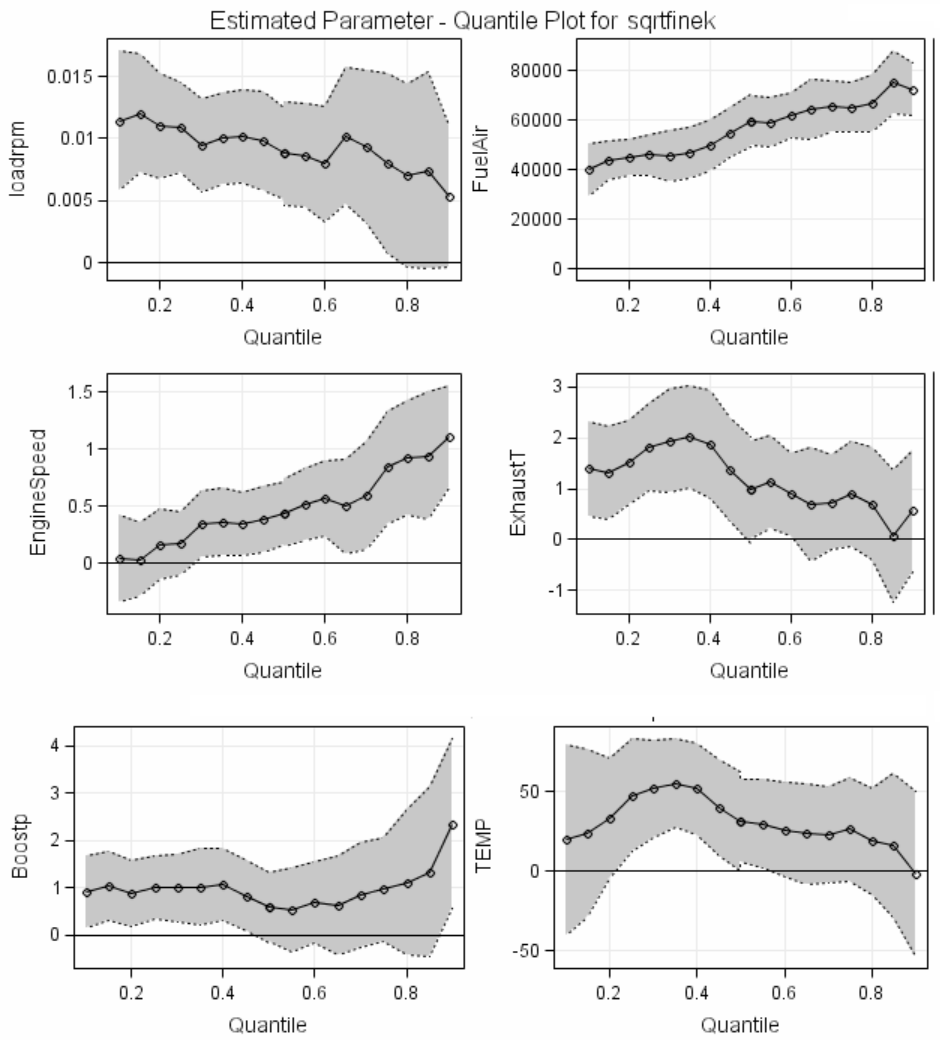


**Figure S-28. Quantile regression process plots for covariate effects on (the square root of) fine particle number rates. The figure corresponds to the second replication of the experiment in Farmington route. A 95% point-wise confidence band for the quantile regression parameters is indicated by the shaded region. The solid horizontal line indicates the null effect.**

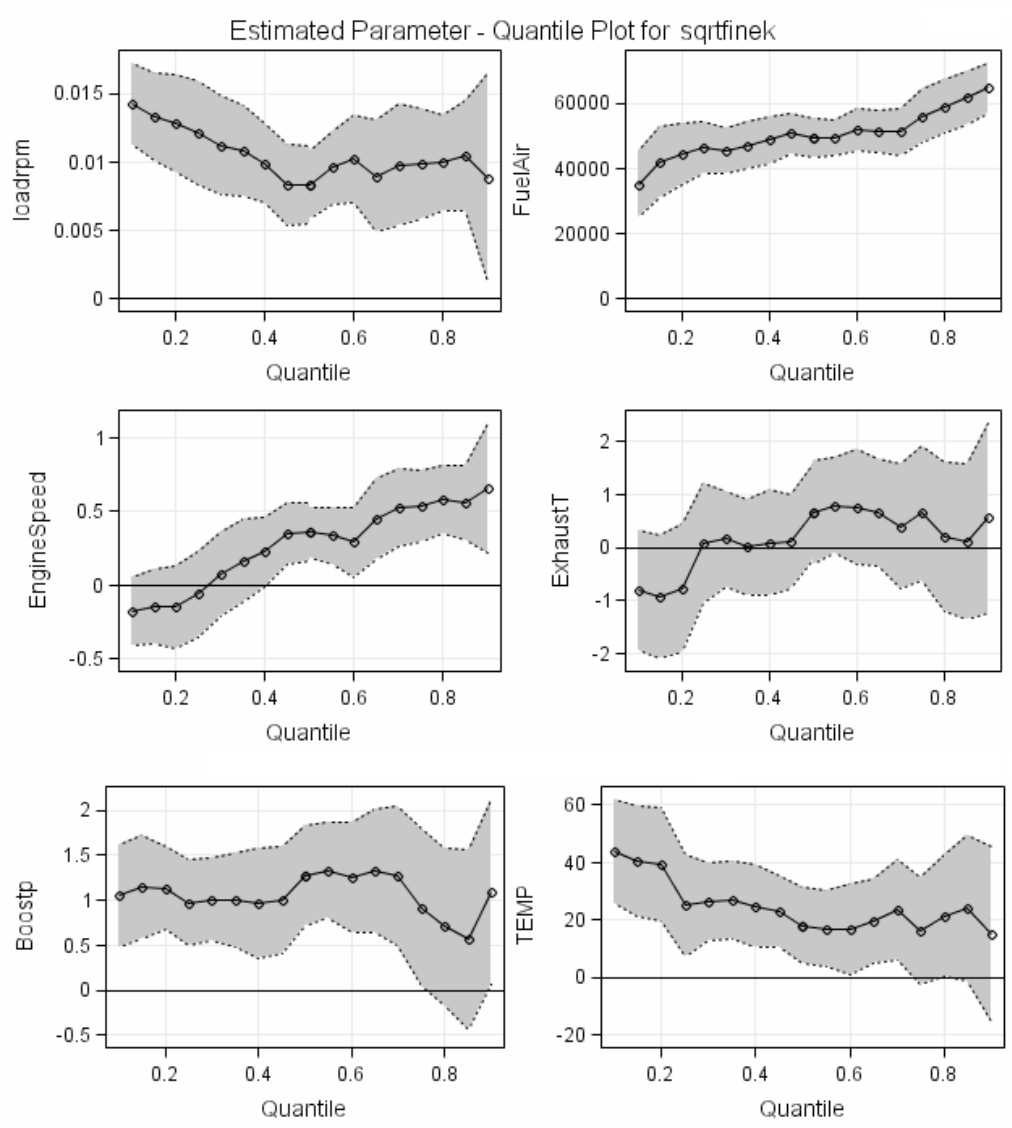


**Figure S-29. Quantile regression process plots for covariate effects on (the square root of) fine particle number rates. The figure corresponds to the third replication of the experiment in Farmington route. A 95% point-wise confidence band for the quantile regression parameters is indicated by the shaded region. The solid horizontal line indicates the null effect.**